ELSEVIER

Coordination Chemistry Reviews 227 (2002) 59–92

COORDINATION CHEMISTRY REVIEWS

www.elsevier.com/locate/ccr

Thermal relaxation in excited electronic states of d^3 and d^6 metal complexes

Leslie S. Forster *

Department of Chemistry, University of Arizona, Tucson, AZ 85721, USA

Received 11 May 2001; accepted 22 October 2001

Contents

* Tel.: +1-520-298-2120; fax: +1-520-621-8407.
E-mail address: forsterl@u.arizona.edu (L.S. Forster).

PII: S0010-8545(01)00458-1

Abstract

Photophysical kinetic results have played an important role in assessing excited state relaxation pathways in transition metal complexes. The applicability of a kinetic analysis is critically dependent on the quality of the individual decay rates, the temperature range examined, and the model used to extract the activation parameters. The extensive literature describing the temperature dependence of excited state depopulation in d^3 and d^6 complexes permits an evaluation of both the power and limitations of kinetic arguments in assessing the mechanism of excited state relaxation.

Keywords: Transition metal complexes; Photophysics; Temperature dependence of decay rates; Environmental mobility and heterogeneity

1. Introduction

A molecule in an electronically excited state differs from one in the ground state in an important way—it must leave the excited state sooner or later. The sequence of processes that follows population of the excited state constitutes the relaxation pathway. This pathway and the rates of the individual processes depend upon intramolecular and extrinsic factors. The possible competitive processes for excited state depopulation include radiative return to the ground state, nonradiative transitions to other states (including the ground state), and chemical reaction (Fig. 1). Temperature is often a very important determinant of the individual rates, either directly or by altering the properties of the environment. Since new channels for excited state relaxation can be opened as the temperature is increased, the overall pathway may change. The measured quantities include the quantum yields of emission and reaction and the emission decay time. Each of these depends on several rate constants and the direct evaluation of the individual rate constants is seldom possible. The variation of the measured quantities with temperature provides additional information about the relaxation pathway.

Transition metal complexes form a class of substances that are useful in assessing the effect of intramolecular and environmental factors on thermal quenching pro-

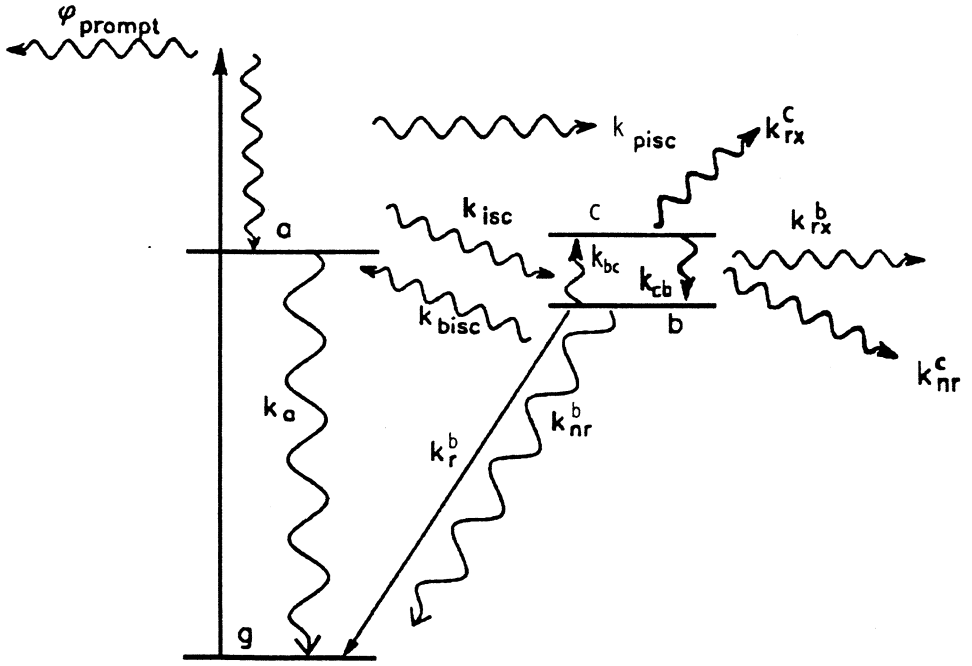

Fig. 1. Schematic energy levels and rate constants. For d^3 complexes, $g = {}^4A_2$, $a = {}^4T_2$, $b = {}^2E$. For d^6 complexes, $g = {}^1A_1$, $a = {}^1T_1$, b and c are ^{3}MC, ^{3}LC, or ^{3}MLCT.

cesses. This is so because both the metal ions and the ligands can be altered, with a concomitant change in the energy levels. It is possible to tune the emission spectrum and excited state properties by appropriate choice of ligands and environment. Furthermore, there is a very large body of results that can be used to suggest general principles that affect decay rates.

After excitation of a transition metal complex, a long-lived level is usually populated. Excited levels can be classified in an approximate but useful scheme in terms of orbital parentage as metal-centered (MC), ligand-centered (LC), and charge-transfer from metal-to-ligand (MLCT) or ligand-to-metal (LMCT). Orbital parentage is essentially a way to describe the difference in electron distribution between the ground and excited states. In MC levels this change is concentrated on the central metal ion. LC levels involve electronic changes in one or more of the ligands and in an MLCT level there is a charge displacement from the metal to a ligand. The ordering of these levels can affect the pathway by which the excitation energy is dissipated.

The preponderance of the extant results are centered on d^3 complexes, mainly Cr(III), and d^6 complexes (Ru(II), Re(I), Os(II), Ir(III), Rh(III), Mo(0), and W(0)). The emission in d^3 complexes is largely MC and arises, for the most part, from intraconfigurational (t_2^3) transitions. In contrast, the emissive levels in d^6 complexes span the entire range of orbital parentage. The thermal behavior of these two groups prior to 1980 has been reviewed [1] The literature in this area has been extensive in the interim but only limited aspects have been surveyed [2–5]. An updated review of thermal effects on excited state relaxation in these metal complexes is now appropriate. The concern here is with intramolecular processes including environmental perturbation; bimolecular quenching and energy transfer between complexes will be ignored. The aim is to identify the factors that mediate the thermally enhanced excited state decays. Although some inferences can be made on the basis of data obtained at a few temperatures, it is much more informative to obtain sufficient quantitative kinetic data to extract activation energies. Since the approach is mainly kinetic, the data quality is a key factor and there will be much emphasis on this feature. Only complexes containing a single metal atom are considered.

2. General principles

2.1. Kinetic analysis

The rate constants in Fig. 1 designate radiative (k_r), nonradiative return to the ground state (k_{nr}), interstate transitions (k_{pisc}, k_{isc}, k_{bisc}, k_{bc}, k_{cb}), and reactive (k_{rx}) processes. The excitation in the spin-allowed manifold $a \Leftarrow g$ can be transferred to b prior to thermalization (k_{pisc}) or from thermalized a (k_{isc}). Not all excited states that may be accessible from b and sublevel splittings are shown. A general treatment for interconversion between all excited levels is possible [6], but a three-level model is often adequate. In this model the relevant levels for d^3 complexes are $g = {}^4A_2$, $a = {}^4T_2$, and $b = {}^2E$. In d^6 complexes $g = {}^1A_1$, b and c are assigned to ${}^3T_1$, ^{3}MLCT, or ^{3}LC. Only processes following population of b are included. The three-level model will first be discussed and the effect of sublevel splitting described later.

The time dependence of the ${}^2E$ population in d^3 systems is given by [7]

$$[{}^2E] = (a_1 \exp(-\lambda_1 t) + a_2 \exp(-\lambda_2 t))/(\lambda_2 - \lambda_1) \quad (1)$$

with

$$\lambda_{1,2} = 0.5[k_a + k_{isc} + k_b + k_{bisc} \mp ((k_a + k_{isc} - k_b - k_{bisc})^2 + 4k_{isc}k_{bisc})^{1/2}] \quad (2)$$

where $k_a = k_r^a + k_{nr}^a + k_{rx}^a$ and $k_b = k_r^b + k_{nr}^b + k_{rx}^b$.

Since $\lambda_2 \gg \lambda_1$ and the emission intensity for ${}^2E \Rightarrow {}^4A_2$ is $I(t) = k_r^b[{}^2E]$

$$I(t) = I(0)\exp(-k_{relax}t) \quad (3)$$

where $k_{relax} = \lambda_1$.

When $k_{isc}k_{bisc}/(k_a - k_b)^2 \ll 1$, a good approximation for k_{relax} is [1]:

$$k_{relax} = (k_b + (1 - k_{isc}/(k_a + k_{isc}))k_{bisc} \quad (4)$$

This is based on the establishment of a steady state for $[{}^4T_2]$ at short times compared with the decay time, which requires that $k_a \gg k_b$.

It has been shown that the efficiency of populating the lowest triplet level is close to unity in d^6 complexes [8], although some exceptions have been claimed [9,10]. Assuming $k_{bisc} = 0$

$$k_{relax} = 0.5[k_c + k_{cb} + k_b + k_{bc} - ((k_c + k_{cb} - k_b - k_{bc})^2 + 4k_{cb}k_{bc})^{1/2}] \quad (5)$$

with $k_c = k_{nr}^c + k_{rx}^c$. For d^6 complexes, the steady-state condition, $(k_{bc}k_{cb}/(k_c - k_b)^2) \ll 1$, leads to

$$k_{relax} = k_b + (1 - k_{cb}/(k_c + k_{cb}))k_{bc} \quad (6)$$

The validity of this equation is dependent upon $k_c \gg k_b$.

When the interconversion rate between ${}^4T_2$ and ${}^2E$ is fast enough to establish a near Boltzmann distribution, a quasi-equilibrium condition obtains and Eq. (4) is replaced by

$$k_{relax} = \tau^{-1} = \frac{k_b + k_a \cdot k_{bisc}/k_{isc}}{1 + k_{bisc}/k_{isc}} \quad (7)$$

for d^3 complexes. An analogous expression can be written for fast interconversion between b and c. This equation has been generalized to describe the population decay of manifolds containing any number of states in equilibrium [11].

The absolute emission quantum yield is the fraction of absorbed photons that is reemitted. The relation between the measured yield and the individual rate constants is [233]:

$$\Phi_{em} = \frac{\text{quanta emitted}}{\text{quanta absorbed}} = \eta_b \eta_{em} \quad (8)$$

where η_b is the fraction of absorbed quanta that reaches b and includes recycling between a and b for d^3 complexes and c and b for d^6 complexes. $\eta_{em} = k_r^b/(k_b + k_{bc})$ for d^6 and $\eta_{em} = k_r^b/(k_b + k_{bisc})$ for d^3 complexes. $\eta_{bc} = k_{bc}/(k_b + k_{bc})$; $\eta_{cb} = k_{cb}/(k_c + k_{cb})$; $\eta_{isc} = k_{isc}/(k_{isc} + k_a)$; $\eta_{bisc} = k_{bisc}/(k_{bisc} + k_b)$.

The radiative rate for $b \Rightarrow g$ can be evaluated from

$$\Phi_{em}/\tau = n'_b k_r^b \quad (9)$$

where η'_b designates the fraction of the absorbed quanta that reaches b on the time scale of the a decay.

The measured Φ_{rx} is the sum of prompt reaction before thermalization and the delayed reaction [233]:

$$\Phi_{rx}(\text{delayed}) = \eta_b(\eta_{rx}^b + \eta_{bisc}\eta_{rx}^a)(d^3)$$

$$\Phi_{rx}(\text{delayed}) = (\eta_{rx}^b + \eta_{bc}\eta_{rx}^c)/(1 - \eta_{bc}\eta_{cb})(d^6) \quad (10)$$

The delayed reaction contains contributions from direct reaction in b and reaction in any level that is thermally accessible (a or c). ϕ_{rx}^b represents the primary (not necessarily the overall) quantum yield for reaction from b, and by analogy to Eq. (9):

$$\phi_{rx}^b/\tau = \eta'_b k_{rx}^b \quad (11)$$

2.2. Thermal contributions to the decay rate

The overall depopulation rate of b can be partitioned into temperature dependent and independent contributions

$$k_{relax} = k_0 + k(T) \quad (12)$$

where $k_0 = k_r^b(0) + k_{nr}^b(0)$ is the low temperature decay rate.

If the radiative rate is temperature independent, the steady state limit for b yields:

$$k(T) = k_{nr}^b(T) + k_{rx}^b + (1 - \eta_{isc})k_{bisc} \quad (13)$$

for d^3 complexes and

$$k(T) = k_{nr}^b(T) + k_{rx}^b + (1 - \eta_{cb})k_{bc} \quad (14)$$

for d^6 complexes. In general

$$k_{relax} = k_0 + \sum A_i \exp(-E_i/k_B T) \quad (15)$$

The number of terms in the summation that are meaningful is limited by the data quality (see Section 2.4). In addition, there is always a question of the physical interpretation of the parameters in a multiexponential fit.

Another limit applies when quasi-equilibrium obtains between two or more excited states (Eq. (7)). For three non-degenerate states, j, k, and l, where j is the lowest excited state and ΔG_k and ΔG_l are the free energy differences between j and the other two states, respectively [11].

$$k_{relax} = \frac{k_j + k_k \exp\left(\frac{-\Delta G_k}{k_B T}\right) + k_l \exp\left(\frac{-\Delta G_l}{k_B T}\right)}{1 + \exp\left(\frac{-\Delta G_k}{k_B T}\right) + \exp\left(\frac{-\Delta G_l}{k_B T}\right)} \mathfrak{A} \quad (16)$$

If entropy differences are negligible $\Delta G = \Delta E_i$. When the denominator in Eq. (16) is near unity, Eq. (15) and Eq. (16) will fit the data equally well, but the interpretation of E_i will differ in the steady state and equilibrium limits [136].

2.3. Data collection and analysis

2.3.1. Excited state decay

Measurements of the excited state depopulation rates can be made with pulsed or modulated steady excitation sources. The first lifetime estimates were made on ruby in 1867 by means of chopped radiation with what is now called a phosphoroscope [13]. Modern versions of this method are still used occasionally [14]. Phase modulation measurements of excited state decay are common in measurements of organic and biological molecules [15], but this method is seldom employed for measurements of transition metal complexes. Most of the decays from excited states of transition metal complexes have been obtained with pulsed excitation and the discussion of data collection will be confined to this procedure.

Two methods have been employed for recording decays, current sampling and time-correlated photon counting. In the 1970s, the availability of N_2 lasers made detection of submicrosecond decays by current sampling much easier than had been possible with flashlamp excitation. Prior to 1980, most pulsed measurements were made by photographing an oscilloscope screen following a single excitation pulse. The traces were then 'digitized' by hand, a procedure that limited the data quality. The introduction of transient recorders that transferred the digitized output to a computer facilitated signal averaging of multiple excitation events by the current sampling method. The signal to noise ratio was thereby significantly improved.

High repetition rate pulsed sources, especially dye lasers, coupled with the fast instrumentation developed for nuclear particle research, led to the use of time-correlated single photon counting detection [16]. This method can produce the highest quality data and is recommended for extracting the parameters in nonexponential decays.

Regardless of the data collection method, there must be an analysis procedure that yields physically mean

ingful quantities. The data are represented as $y = f(a_r, x)$ and the aim is to extract the parameters, a_r, by a least-squares algorithm. The first step is to assume a function relating the measured y_i, x_i pairs. This function, also called the model, can be linear or nonlinear in the parameters, a_r. An example of a linear model is $y = a_1 + a_2x + a_3x^2$, while $y = a_1\exp(-a_2x) + a_3\exp(-a_4x)$ is nonlinear. In general,

$$I(t) = \sum I_i(0)\exp - (t/\tau_i) \quad (17)$$

In both the steady state and equilibrium limits, a single term is sufficient no matter how many competing processes are involved. Nonexponential decay requires additional terms to fit the decay. This problem is discussed in Section 2.4.

A single term function can be linearized, but baseline errors are reduced by a nonlinear least-squares fit of $I(t) = B + I(0)\exp(-k_{relax}t)$.

No closed solution exists for a nonlinear least-squares fit. Instead, an iterative procedure is used. Different algorithms are available (Simplex, Marquart–Levenberg, and Gauss–Newton) to make the search efficiently [17,18]. There is no unambiguous test for the applicability of a given model. Both systematic and random errors will affect the goodness-of-fit. The correlation between parameters makes fitting of multiexponential models uncertain unless the exponential factors are more than twofold different. At the very least, the fit must be the same over a wide range of initial parameters. This will ensure that a global rather than a local minimum has been reached.

2.3.2. Emission spectra

When recorded under steady illumination, an emission spectrum is obtained by scanning over the wave length range where the emission intensity is appreciable. If the monochromator-detector sensitivity varies markedly over this range, it is desirable to calibrate the detection system against some standard that has a known spectral distribution. The corrected spectrum represents a time integral:

$$I(\lambda) = \int_0^\infty I(\lambda,t)\mathrm{d}t \quad (18)$$

Time-resolved emission spectra are recorded by time gating with a box-car integrator. The monochromator is then scanned with a predetermined delay time (Δt). This provides $I(\lambda,\Delta t)$.

2.3.3. Emission quantum yields

The relative quantum yield can be determined by measuring quanta emitted/quanta absorbed for the sample and some reference material. Artifacts that must be considered in quantum yield measurements have been reviewed [19]. These include corrections for refractive index, reabsorption of emission, and polarization.

In order to use Eq. (9) for the calculation of radiative rates, absolute emission yields must be evaluated. If a standard with a known absolute yield is used, the relative quantum yield can be converted into an absolute yield. Methods have been developed for determining absolute yields that do not depend on the use of a reference with a known yield [19].

2.4. Nonexponential excited state decay

Assessment of any deviation from exponentiality is important in two areas: (1) establishing the rate of population decay in the excited state; (2) relating the extent of nonexponentiality to physically meaningful inferences such as connecting environmental heterogeneity to the thermal decay pathway. More importantly, significant deviations from exponential decay would invalidate the use of Eq. (15) to extract thermal activation parameters.

Observed deviations from exponentiality can be real or artifactual. Artifacts include baseline errors, emission from lenses and dewars, scattered excitation light, temperature inhomogeneity, impurity luminescence (including photoproduct emission), as well as polarization and emission spectral changes during the decay. As data collection methods become more precise, smaller deviations from exponentiality will be detectable, but it is risky to reach conclusions based on small effects, which can be artifactual.

No foolproof method exists for detecting impurity emission, but several strategies are useful. The most obvious approach is to record the decay after successive attempts at purification. The lifetimes of the impurity and the genuine emission usually differ. The emission spectrum would then vary with the delay time in a time-resolved spectrum, but environmental heterogeneity can also lead to spectral changes with delay time. The variation in the emission characteristics with excitation wave length can also be informative. Alternatively, marked dependence of the emission spectrum on temperature may be an indicator of impurity emission, but there are many examples of genuine emission exhibiting such a change.

When the emission is highly polarized, molecular rotation during the decay will introduce nonexponentiality in the emission decay even when no polarizers are used in the detection system [21]. For microsecond lifetimes, polarization artifacts will only be significant at low temperatures where the solvent is very viscous. Few lifetime reports have explicitly considered the polarization effect. The $Re(CO)_3(phen)Cl$ emission is highly polarized, yet the emission decay is exponential in a solution where molecular rotation competes with decay [22]. Polarized ^{3}MLCT emission has been observed [23,24].

If deviations from exponentiality are due to environmental heterogeneity in a glass or supercooled liquid (Section 2.5), the decay should become exponential when solvent motion is much faster than the excited state decay. Persistence of nonexponentiality in the fluid is evidence for impurity emission. However, multiple emission might also lead to nonexponentiality (Section 2.9).

Spectral changes with delay time will generally lead to artifactual nonexponentiality when measurements are recorded at a specific emission wave length. The decays in $Ru(bpy)_3^{2+}$, collected by the highly precise time-correlated single photon counting procedure and analyzed by a weighted non-linear least-squares treatment, yielded a good single-exponential fit at temperatures where time dependent spectral shifts prevail [46]. This puzzling observation was addressed by recording the emission at different emission wave lengths [25]. The expected deviations from exponentiality were detectable at most wave lengths, but at a particular wave length the fast decay component became negligible and exponentiality obtained. At longer wave lengths, a rise-time was observed. When the entire emission was monitored, $I(t)$ decayed exponentially.

In principle, the decays can always be fit to Eq. (17) and the relative magnitudes of $I_i(0)$ will indicate the extent of nonexponentiality. Not even the highest data quality will yield an acceptable fit if more than three terms are required and two-exponential fits may not be physically meaningful. The stretched exponential function, $I(t) = I(0)\exp(-(t/\tau_0)^{\beta})$ has been used for fitting nonexponential data [26–28]. The reduction of β from unity is a measure of nonexponentiality, but the stretched exponential function has rarely been used to describe excited state decays [28]. The time for $I(t) = I(0)/e$ is often used as an average 'lifetime'. Other averages that have been used are $\langle t \rangle = \int I(t)dt/I(0)$ and $\bar{t} = \int tI(t)dt/\int I(t)dt$ [29], but these do not provide a quantitative estimate of the deviation from exponentiality. An arbitrary measure of relative deviations from exponentiality has been used to assess the effect of solvent mobility on excited state decay [26].

2.5. Environmental heterogeneity

A common source of intrinsic deviations from exponentiality is environmental heterogeneity. The kinetic analysis presented in Section 2.1 refers to a collection of complexes in the same environment. An ideal environment would be a perfect crystal in which all complexes occupied crystallographically identical sites. Under these conditions, the excited state decay would be strictly exponential.

When solvent motion is fast on the time scale of the emission decay, each complex is in the same average environment and the decay is exponential. At the other extreme, as in a rigid solution, a multitude of environments are frozen-in and the decay should be nonexponential unless k_{relax} is the same in all environments. It is remarkable that very good exponentiality is observed in rigid solutions of many complexes at low temperatures, indicating the insensitivity of k_0 to environmental heterogeneity in those cases.

If all the complexes are in a crystal where the environments are identical, a spectral feature is a superposition of rovibronic lines, each homogeneously broadened. The line width in a homogeneously broadened line in the emission spectrum would be much less than 1 cm^{-1} [30]. Homogeneous broadening in higher vibrational levels is increased by relaxation. In practice, the emission lines are broadened inhomogeneously by small variations in the environment even when all of the complexes are in crystallographically identical sites. Inhomogeneous broadening in an amorphous medium is much larger, and can exceed 1000 cm^{-1}.

The consequence of inhomogeneous broadening is most significant when two electronic states are proximate. In that case, the relative disposition of the two levels can vary from one complex to another. There can be a broad distribution of energies due to the site inhomogeneity. This, in turn, would be reflected in the dependence of the time-resolved spectrum with delay time and deviations from exponential decay. The possible overlap of broad distributions is central to the analysis of multiple emission (Section 2.9).

2.6. Thermal activation parameters

The aim of determining $k(T)$ is to extract activation parameters and thereby to infer the relative importance of the several pathways for the depopulation of excited states. A quantitative approach to this analysis involves fitting Eq. (15) for the steady state limit or Eq. (16) in the equilibrium limit.

As in the case of fitting excited state decays by Eq. (17), the application of either of these equations is limited by the data quality. Compared with the decay rate case, fewer data points are usually available in the fitting of the thermal decay parameters. The paucity of data limits the reliability of the fit when statistical techniques based on the least-squares criterion are employed. Good statistical fits require that the data set be overdetermined with many more data points than parameters. Furthermore, the temperature range is often small and the reliability of the extracted A_i and E_i values is limited. The preponderance of the literature results was obtained with one or two-exponential models, and the assessment of model adequacy is important. There is sometimes a concordance between the high temperature E_i obtained in a two-exponential fit with the value obtained in single-exponential fit, but not always.

An example of a complex in which the least-squares fit can be misleading is $Ru(bpz)_2(bpy)^{2+}$ [31]. A single-exponential model yielded $E = 1859\ cm^{-1}$ in the temperature range 243–330 K. When the upper temperature was increased to 373 K, a two-exponential model produced activation energies of 4632 and 736 cm^{-1}. Only by increasing the temperature range was the higher activation energy process revealed.

Prerequisite to applying Eq. (15) is a good fit of k_{relax} to an adequate model at each temperature. If a single term model is assumed for Eq. (17), the decays must be exponential. In principle, two-term fits of the decays could yield two $k(T)$ values, but this presumes such a fit yields physically meaningful values. Failure of $k(T)$ to conform to a single term in Eq. (15) (Arrhenius behavior) [32] may be due to the nonexponential character of the excited state decay or to competing thermal relaxation pathways [33].

The interdependence of A and E also indicates that caution should be exercised in making inferences based upon activation energy differences. Near room temperature (r.t.) an order of magnitude change in A is equivalent to a 5 kJ mol^{-1} (400 cm^{-1}) change in E. Furthermore, nonlinear least-squares fitting may lead to different results, depending upon the convergence criterion, the least-squares algorithm, and the presence of local minima. This problem is exemplified by a fit of the *trans*-$Cr(cyclam)(NH_3)_2^{3+}$ lifetime data in [34], which yields $E = 56$ kJ mol^{-1} [35] instead of the published 73 kJ mol^{-1} value.

2.7. Nonradiative transitions

The $k_{nr}(0)$ component of the nonradiative rate, $k_{nr} = k_{nr}(0) + k_{nr}(T)$, is treated theoretically in the weak-coupling limit where the geometry differences between the ground and emitting states is small [246]. Application to transition metal complexes has been made [247,251]. In the weak-coupling limit, nonradiative processes involve tunneling between the two surfaces and a useful approximation is

$$k_{nr}(0) = \beta F \quad (19)$$

where β is the electronic factor that involves promoting modes and F represents the overlap of accepting vibrational functions between the initial and final electronic states [36]. The major contribution to F is ΔE, the energy difference between the two state origins. This leads to an energy gap dependence, wherein $k_{nr}(0)$ decreases exponentiality with ΔE. The energy-gap law has been validated [37–39], but changes in β cannot be ignored [87,111].

$k_{nr}(T)$ has also been treated in the weak coupling limit and an Arrhenius dependence was predicted [40]. A linear relation between $\ln k_{nr}$ and T was derived by Claude and Meyer [36,45]. The temperature dependence is very small for both complexes, which are ^{3}MLCT emitters. There is less than a 50% increase in k_{nr} over a 90° temperature interval.

The weak coupling limit does not apply to activated surface crossing and large changes in $k(T)$ cannot be attributed to tunneling unless solvent motion reduces the energy gap. In weak coupling, the largest contributions to F come from the high frequency modes since fewer accepting mode quanta are needed to span the energy gap. The high frequency stretching NH and OH modes are often the major accepting modes [87,111,252]. The frequencies of these modes are decreased by deuteration and the larger number of quanta required to dissipate the excitation energy leads to a decrease in $k_{nr.}$ No deuterium effect is expected when weak coupling is not obtained.

2.8. Solvent motion, emission spectra and excited state decay

The effect of environmental mobility on the emission depends upon the relative time scales of τ_s, the correlation time for solvent mobility, and t_m, the measurement time. τ_s can be measured by dielectric and light scattering techniques [214] and many solvents have been characterized as a function of temperature. In decay and steady excitation emission spectral measurements, t_m is the excited state lifetime, τ. When time resolved spectra are recorded, t_m is the delay time, Δt. Three solvent motional domains can be distinguished; fast, $t_m > \tau_s$; intermediate, $t_m \approx \tau_s$; and slow, $t_m < \tau_{s.}$

Relevant solvent motions are translation, rotation, and side chain movement. At any instant there is a distribution of solvent environments around the solute molecules. Each solvent disposition can be characterized as a solvate species. In a rigid medium, there is no change in the solvates with time. The spectral and kinetic properties vary from one solvate to another. As solvent motion becomes significant on the timescale of the excited state lifetime, interconversion between the solvates occurs. Two effects of such motion can be distinguished. In one case, there is a difference in polarity between the ground and excited levels as in the $^3MLCT \leftarrow {}^1A_1$ transition. At the instant of excitation the excited and ground state solvates are the same. Due to the polarity change, there will be a free energy difference between the equilibrium distributions in the two levels. In a rigid medium no relaxation is possible, but in a fluid there is a driving force toward lowering the free energy in the excited level by solvent rotation [132]. The result will be a shift in the emission spectrum to longer wave lengths. The redshift is due to a reduction in the $^3MLCT-{}^1A_1$ energy gap and there is a concomitant increase in $k_{nr}(T)$. At higher temperatures thermal motion reduces the interaction and the ^{3}MLCT energy is increased [46]. If there is an abrupt change in

solvent mobility with temperature both $k_{nr}(T)$ and wavelength will exhibit a plateau after the first sharp change, but in some cases only an inflection occurs [20,52]. These phenomena are observed in the relaxation of Ru(II) ^{3}MLCT levels [45,46,51].

Changes in energy levels that accompany the transition from the slow to the fast regimes have been termed rigidochromic [41]. Many putative rigidochromic effects have been observed at only two temperatures; low (slow) and high (fast). Thermal population of higher levels can also contribute to the spectral changes. In order to separate thermal from solvent mobility effects, the spectral shifts must be correlated with solvent mobility. Purely thermally induced spectral changes have been observed in solids [42,43].

Rigidochromism has also been observed in the emission of some quadrate d^3 complexes [44]. It is generally assumed that ^{3}LC and ^{3}MC emission will not exhibit rigidochromism, but several examples of spectral redshifts in supposed ^{3}MC emission from Rh(III) and Ir(III) complexes have been found [48,49]. There is a rigidochromic shift in the d–d absorption band of $Cr(acac)_3$ [50].

In the second class of solvent mobility effects, exemplified by MC levels, there is no free energy difference to drive changes in the excited state. The structure of each solvate can affect the shape of potential surfaces as well as the solute energy levels. In particular, there is a viscosity effect on the potential surface anharmonicity [248,249]. In a rigid medium there is no interconversion between solvates. If there are different decay rates among the solvates, the decay will be nonexponential in the rigid environment. Solvent motion in this context means fluctuations that correspond to solvate interconversion. In the fast solvent motion limit each complex will sense the same average environment and the decay becomes exponential.

It is the range between the fast and slow limits that is interesting. In this domain the solvate interconversion rate permits the excited complex to sample a range of species and in an activated process those solvates with the fastest relaxation rate will dominate $k(T)$. In Cr(III) complexes fluctuations could influence $k_{nr}(T)$ or $k_{bisc.}$ The source of the relaxation rate variation among the solvates is a question, which will be addressed below.

2.9. Energy transfer, localization, and multiple emission

When the emitting level is metal-centered, as in d^3 complexes, the main effect of electron delocalization onto the ligands is the reduction of electron repulsion with the concomitant shift of the emission to longer wave lengths [50].

There have been long-standing controversies about the extent to which ^{3}MLCT and ^{3}LC excitations in d^6 complexes are localized in individual ligands [53–55]. In the localized model, the ^{3}MLCT or ^{3}LC emission originates in an excited level associated with the ith ligand rather than with more than one ligand. If the ligands in a homoliganded complex are in identical environments, there are three equienergetic-localized levels. When the transfer rate is very fast, an exciton (delocalized) description is appropriate. Otherwise, the excitation is said to be more or less localized. The conditions for delocalization in crystalline hosts have been detailed and localization does not imply absence of energy transfer between ligands [56]. It was concluded that the excitation is localized in $Ru(bpy)_3^{2+}$ but delocalized over the entire complex in $Os(bpy)_3^{2+}$ [57,58]. The localized model for $Ru(bpy)_3^{2+}$ excitation in crystals at low temperatures has been challenged [59,60].

Even in a crystal the three ligands in a homoliganded complex need not be in equivalent sites and the energy identity would then be destroyed. If energy transfer is fast on the emission time scale, but still localized, the excitation would lead to population of the lowest level or to levels that are thermally accessible from it.

Much of the controversy about localization results from an analysis of very low temperature spectra of complexes in crystalline environments. Though there is disagreement about the appropriate description in crystals, it is generally agreed that localization is obtained in glassy hosts where each ligand environment is different and the separation between the localized levels is substantial. The excitation is then localized on the ligand with the lowest energy.

The most direct evidence for localization in $Ru(bpy)_3^{2+}$ and $Os(bpy)_3^{2+}$ at ambient temperatures in fluid media comes from excited state time-resolved Raman spectra [61–63]. These spectra are consistent with $Ru^+(bpy)_2(bpy^-)^{2+}$ as the structure in the ^{3}MLCT level. The rate of interligand energy transfer depends upon τ_s [64]. The dynamic nature of the localization in fluid solutions of $Ru(bpy)_3^{2+}$ has been demonstrated [232]. The excitation is initially delocalized but becomes localized in less than a picosecond. Other evidence supporting the localized model has been summarized by Kalyanasundaram [65].

Crosby suggested long ago that "emission from a transition-metal complex with an unfilled d shell will occur from the lowest electronic state in the molecule or from those states that can achieve a significant Boltzmann population relative to the lowest excited state" [118]. This rule implies that energy transfer rates between excited levels is faster than decay to the ground state. It is useful to distinguish interligand energy transfer between levels of the same orbital parentage (^{3}LC $\Rightarrow$ ^{3}LC and ^{3}MLCT $\Rightarrow$ ^{3}MLCT) from transfer between levels of different orbital parentage. If transfer of either type is sufficiently slow to prevent thermalization prior to decay, multiple emission can be observed. Some

authors term this dual emission, while others describe emission from two thermally equilibrated levels as dual.

In heteroliganded complexes, where the energies of the levels localized in different kinds of ligands are no longer the same, the Crosby rule implies that energy transfer should lead to localized emission from the ligand with the lowest excited level, as observed [181]. Although this model is important in systematizing the ^{3}MLCT and ^{3}LC excited state relaxation results, a number of exceptions have been claimed. An apparent case of slow interligand transfer between localized ^{3}LC levels was apparently observed in glassy solutions of $Rh(bpy)_n(phen)_{3-n}^{3+}$. The decay was exponential in the homoliganded pair but nonexponential in the heteroliganded complexes [67]. This result was interpreted to indicate ^{3}LC localized emission from both phen and bpy when $n = 1$ or 2. Instead of multiple emission, the nonexponentiality has been attributed to inhomogeneous broadening in the glass due to environmental heterogeneity [68]. The energy difference between the localized phen and bpy excited states is small enough to ensure overlap between the phen and bpy inhomogeneously broadened energy levels. The phen energy is then the lowest excited state in some complexes and the bpy energy the lowest in others. The observed decays were due to a superposition of emission from different complexes [30].

Multiple emission has been associated with inhibition of thermal communication between energy levels of different orbital parentage. The emission from several $Ir(NN)_2Cl_2^+$ complexes has been interpreted as multiple in that the higher ^{3}MLCT or ^{3}LC levels do not relax readily to the lower ^{3}MC levels [73–76]. The specific model proposed for *cis*-$Ir(bpy)_2Cl_2^+$ in which the ^{3}MLCT level is 370 cm^{-1} above ^{3}MC [73] has been questioned, but multiple emission was not rejected [69]. Two emission bands with lifetime dependence on the monitoring wave length have been observed in a heteroliganded Ru(II) complex [70]. The emission is strong in both regions and is invariant to sample preparation. Interlevel conversion is inhibited by solvent rigidity [69].

Most examples of supposed multiple emission were observed in rigid media and are probably due to environmental heterogeneity, as evidenced by the rarity of such emission in fluids. Multiple emission in a fluid medium has been claimed for $Ru(bpy)_2(pztr)^+$ [70] and for some Re(I) complexes [71]. It is difficult to distinguish unambiguously between a real failure to achieve intramolecular thermalization from the effect of environmental heterogeneity [72]. This problem will be examined again in the sections dealing with d^6 complexes, but it appears that multiple emission is rare in Ru(II), Os(II), Rh(III), and Ir(III) complexes. It is only in Re(I) complexes that many examples of multiple emission have been described, and usually the nonexponentiality disappears in the fluid.

Nonthermalization between the emissive level and a non-emissive level has been suggested in $Ru(bpy)_2(dmpbq)^{2+}$ [9].

Since most claimed examples of multiple emission have been ascribed to environmental heterogeneity that leads to inhomogeneous broadening of excited levels [68,78], it has been asserted that no genuine case of multiple emission exists [30].

3. Cr(III) complexes

Kirk has reviewed the photochemistry and photophysics of Cr(III) complexes in some detail [5]. His main conclusions that bear on the present discussion are:

1. $^4T_2$ is the photoactive level in many (most?) complexes.
2. Stereochemical change usually accompanies photoreaction.
3. Back-intersystem crossing is the major thermal relaxation pathway in all but a few complexes.
4. The best estimate of the $^4T_2$–^{2}E gap in a fluid medium is the activation energy for ^{2}E depopulation.

3.1. Energy levels

Fig. 1 serves as a starting point for the kinetic analysis of d^3 complexes. The *b* (^{2}E) energy is not sensitive to the ligand field strength of the coordinated ligands, but will be reduced when the metal d electrons are delocalized onto ligands that have low-lying empty π* orbitals ($acac^-$, CN^-) [50].

The *a* ($^4T_2$) energy varies with the ligand field strength of the coordinated ligands. Consequently, both the $^4T_2$–^{2}E 0–0 energy difference (ΔE) as well as the $^4T_2$–^{2}E crossover energies vary markedly from complex to complex. The estimation of ΔE from spectra has proven to be unreliable. The ^{2}E energy is readily evaluated from the sharp $^2E \Rightarrow {}^4A_2$ emission spectrum. In the absence of $^4T_2 \Rightarrow A_2$ fluorescence, the $^4T_2$ energy can only be estimated from the broad $^4T_2 \Leftarrow {}^4A_2$ absorption spectrum. Rarely is the origin of $^4T_2 \Leftarrow {}^4A_2$ resolved and it is difficult to determine the $^4T_2$ energy from the absorption spectrum. One exception is $Cr(NH_3)_6^{3+}$ in a crystal where the origin has been located at 501 nm [250]. A number of methods have been suggested for the determination of the $^4T_2$ origin but none have been validated [79].

In most complexes, $^2E \Rightarrow {}^4A_2$ emission occurs in the 660–720 nm region [7], but delocalization onto the ligands can shift the spectrum to 800 nm. The sharp $^2E \Rightarrow {}^4A_2$ emission is indicative of very little geometry

change between the ground and excited states as expected for an intraconfigurational (t_2^3) transition. Broad $^4T_2 \Rightarrow {}^4A_2$ ($t_2^2e \Rightarrow t_2^3$) fluorescence is not observed at very low temperatures when $^4T_2$ is above ^2E, the usual situation in Werner complexes. When fluorescence is detectable, the emission bands are broad [29,80].

The ^2E splittings can be as large as 200 cm^{-1} in tetragonal fields [82], but are usually smaller. The $^2T_1$ splitting increases with the tetragonal field strength and one of the components can be driven below ^2E [83]. The splitting of the $^4T_2$ levels in low symmetry fields can be substantial. $^4T_2$ is subject to Jahn–Teller distortion [250].

3.2. Thermal relaxation pathways

Identification of the thermal relaxation pathways for many Cr(III) complexes has been a continuing problem [2,7,84]. Each of the three contributions to $k(T)$ in Eq. (13) corresponds to a process that can depopulate ^2E. These processes are: direct ^2E reaction (k_{rx}^E), back-intersystem crossing to $^4T_2$ (k_{bisc}), and enhanced nonradiative return to the ground state or to some intermediate species ($k_{nr}^E(T)$). All of these can lead to product formation, but chemical reaction need not be directly related to depopulation of ^2E, since reaction can occur in $^4T_2$ prior to population of ^2E. Even the absence of photoreaction does not exclude k_{rx}^E because geminate recombination can reduce Φ_{rx}. A good fit by a single term Arrhenius function indicates the dominance of one relaxation channel.

In spite of the uncertainty in the magnitude of the $^4T_2$–^2E gap, it is possible to identify complexes in which the k_{bisc} contribution is energetically allowed. There are some complexes in which $^4T_2$ is only slightly above ^2E and is thermally accessible at moderate temperatures. In one of the first reports of luminescence from a Cr(III) complex both fluorescence and phosphorescence from $Cr(urea)_6^{3+}$ were observed in a glass at 87 K [85]. The fluorescence increases relative to the phosphorescence as the temperature is raised, indicating that back-intersystem crossing leads to $^4T_2 \Rightarrow {}^4A_2$ emission [86]. However, thermally induced delayed fluorescence is rarely detectable even when $^4T_2$ is populated because k_r^T can be much smaller than k_{nr}^T.

The effect of ligand field strength on the $^4T_2$ energy is exemplified by the $Cr(NH_3)_{6-n}(H_2O)_n^{3+}$ series, where the onset temperature for $k(T)$ decreases with n [87]. The phosphorescence emission position is hardly affected by n, but the reduction of the $^4T_2$–^2E gap is evidenced by the weak fluorescence in $Cr(D_2O)_6^{3+}$ [88].

The activation energy for $k(T)$, E, must be at least as large as the energy difference between the $^4T_2$ and ^2E origins, ΔE, for k_{bisc} to contribute significantly to ^2E depopulation. In the limit of quasi-equilibrium between $^4T_2$ and ^2E, $E = \Delta E$. In the steady state limit, the activation energy of k_{bisc} reflects the energy to reach the crossover between the $^4T_2$ and ^2E potential surfaces rather than the energy difference of the minima must be at least as large as ΔE.

By varying the $^4T_2$–^2E gap, solvent mobility, and temperature, the contribution of back-intersystem to the thermal decay pathway can be inferred [26,94]. The salient points are: (i) when the $^4T_2$–^2E energy difference is small, thermal quenching begins in rigid media and is accompanied by significant nonexponentiality, indicating a distribution of E values in the solvates. Increasing the $^4T_2$–^2E gap increases the temperature at which nonexponential decay is observed; (ii) as ΔE increases $k(T)$ becomes important only when solvent motion is either comparable to or faster than excited state decay. Changing the solvent alters the temperature at which τ_s approximates τ. Solvent motion is assumed to lower the $^4T_2$–^2E crossover energy by changing the potential energy surface (PES) [248,249]; (iii) when ΔE is large $k(T)$ occurs only when the solvent is very mobile. For these complexes, it becomes difficult to find solvents that are immobile at the higher temperatures required for $k_{nr}(T)$. However, embedding large ΔE complexes in a crystalline host suppresses thermal decay.

Steric effects on energy levels may be characterized as static and dynamic. Static distortions involve departure of the skeletal framework from near-octahedral symmetry and are detectable by X-ray crystallography. The ^2E energy is only slightly affected by a static distortion [79] and there is no driving force for a geometry change in the ^2E level when a rigid environment becomes mobile. There is some evidence from absorption spectra that the energy of one $^4T_2$ component is reduced by large static distortions [79]. The absorption in a highly substituted strained $Cr(en)_3^{3+}$ derivative is markedly redshifted [89]. Dynamic distortions are changes that are permitted by solvent movement on the timescale of the ^2E decay and reduce the $^4T_2$–^2E crossover energy. An abrupt increase in $k(T)$ in the temperature range where environmental constraints are relaxed is the evidence that dynamic distortions are involved.

The low temperature limiting decay rates for many Cr(III) complexes have been reported [7]. Quantitative analysis of the thermal behavior has been less extensive. Typically, there is a small thermal increase in k_{relax} at low temperature ($E \leq 5$ kJ mol^{-1}) followed by a large increase at higher temperatures. Most of the results in Table 1 have been obtained by single-exponential fits in the high temperature region. The scatter in the E values for a particular complex indicates that inferences based on small differences are risky. Some of this scatter may be due to poor fits to a one-term (Arrhenius) model [32,33]. This in turn may reflect deviations from exponentiality in the individual decays. Some of the solvent dependence of the Arrhenius parameters is due to a compensation between A and E. In solutions of

$Cr(NH_3)_2(NCS)_4^-$, E varies between 40 and 55 kJ mol^{-1} and A from 6×10^{14} to 9×10^{16} s^{-1} [90]. The graph between E and $\ln A$ is called a Barclay–Butler plot; this dependence was originally a thermodynamic one [231]. A linear plot is sometimes assumed to indicate a common thermal decay pathway, but there are exceptions to this generalization. Although entropic contributions can increase A above 10^{14} s^{-1}, pre-exponential factors of 10^{19} s^{-1} are suspect and the result of fitting artifacts or poor data quality.

Chemical reaction can be prompt or delayed. Prompt reaction is not affected by quenching of the ^2E emission and has been observed in rigid and crystalline media [91,92]. Delayed reactions will be reduced by quenching of ^2E as indicated by the effect of O_2 on the Φ_{rx} of $Cr(NH_3)_2(NCS)_4^-$ [92,93]. Whether delayed reaction occurs directly in ^2E, after back-transfer to $^4T_2$, or after leaving ^2E by another nonradiative process such as formation of a ground state intermediate [2] cannot be determined by kinetic measurements alone.

3.2.1. CrN_6 complexes

Complexes in which all six coordination sites are occupied by aliphatic nitrogen atoms have been extensively studied. Arguably, the effort to identify the thermal relaxation pathway in this group has received more attention than other question involving photoprocesses in Cr(III) complexes [79]. This problem arises because the $^4T_2$–^2E gap is on the borderline of permitting back-intersystem crossing to compete with other contributions to $k(T)$; the E values for $Cr(NH_3)_6^{3+}$ and $Cr(en)_3^{3+}$ are in the 41–48 kJ mol^{-1} range with $A = 10^{12}$–10^{14} s^{-1}. $k(T)$ in these two complexes becomes significant only in the fast solvent motion domain when common solvents are involved [94]. The $^4T_2$–^2E gap was accurately determined for $Cr(NH_3)_6^{3+}$ in a crystal as 57 kJ mol^{-1} [250] definitely larger than E. A smaller gap has been estimated in solution and back transfer was assumed to be energetically feasible [253]. The activation energies for $Cr(NH_3)_6^{3+}$ in several solvents in a narrow temperature range near r.t. varied from 46 to 50.6 kJ mol^{-1} [81].

Thermal decay is suppressed when $Cr(NH_3)_6^{3+}$ is embedded in a crystalline host [2]. This might be due to raising the energy of the $^4T_2$–^2E crossover along one or more coordinates. When E is large, it is difficult to find a solvent that is rigid when $k(T)$ becomes appreciable. Sorbitol has a high glass temperature and is very rigid at r.t. The lifetime of $Cr(en)_3^{3+}$ in sorbitol is only reduced from 108 to 98 μs between 77 and 266 K and the decays are nearly exponential. The decay of the same system at 296 K is quite nonexponential with a tail lifetime of 30 μs [26,35]. This shows that the $^4T_2$–^2E crossover in $Cr(en)_3^{3+}$ can be reached without solvent motion, before any change in the potential surfaces.

Back-transfer is consistent with the belief that photoreaction occurs in $^4T_2$ and requires stereomobility [5]. An extensive series of papers by the Endicott group has dealt with the effect of molecular distortion on thermal decay [79,95,97,149]. Static distortions are nearly the same in $Cr(en)_3^{3+}$ and $Cr(sen)^{3+}$ (sen = 4,4′,4″-ethylidynetris(3-azabutan-1-amine)) [95], yet $k(T)$ is 10^4 larger at ambient temperature in $Cr(sen)^{3+}$ [79]. Molecular mechanics calculations indicated that the steric strain could be substantially reduced by a 15° twist in $Cr(sen)^{3+}$ but no such reduction occurs in $Cr(en)_3^{3+}$ [79]. A similar correlation of steric strain and large $k(T)$ was found for two other pairs of complexes. Endicott interpreted the enhanced thermal quenching in a fluid as due to an activated $k_{nr}^{E}(T)$. AOM calculations indicate that changes in geometry along a trigonal twisting coordinate reduces the $^4T_2$–^2E gap and increases the geometry difference between ^2E and $^4A_2$. The gap reduction could enhance k_{bisc}. The activation energy is appreciably smaller in $Cr(sen)^{3+}$ than in $Cr(en)_3^{3+}$. When $Cr(sen)^{3+}$ is doped into $Rh(sen)(ClO_4)_3^{3+}$, the thermal quenching requires a higher temperature [95].

An effect of relaxed distortion on the energy levels is demonstrated by the emission spectra of $Cr(BCNE)^{3+}$ in different environments at 77 K [79]. There is a decrease in the $^2E \Rightarrow {}^4A_2$ energy when the environment is changed from the isostructural $Rh(BCNE)(ClO_4)_3^{3+}$ to rigid DMSO–H_2O, where there is less resistance to reduction of steric strain. The increased $k(T)$ in this complex compared with the value in the related $Cr([9]aneN_3)_2^{3+}$ would then be due to the larger steric strain energy.

The $^4T_2$–^2E gaps, as judged by the $^4T_2$ origin bands in the absorption spectra, are nearly the same in crystalline *trans* and *cis*-$Cr(cyclam)(NH_3)_2^{3+}$, 47 kJ mol^{-1} [98]. In *trans*-$Cr(cyclam)(NH_3)_2^{3+}$ E is 59–67 kJ mol^{-1}. The *cis* complexes, $Cr(cyclam)(NH_3)_2^{3+}$ and $Cr(cyclam)(en)^{3+}$, have much smaller E values, 36–44 kJ mol^{-1} [98]. Since the activation energy is smaller than the $^4T_2$–^2E gap when the *cis* complex is in a rigid environment, it was suggested that the static distortion in the *cis* complex facilitated solvation and led to a $^4T_2$ energy decrease in a fluid medium. This made k_{bisc} the major contribution to $k(T)$.

The suggestion that the thermal decays in *cis* and *trans*-$Cr(cyclam)(NH_3)_2^{3+}$ involve different pathways [99] was based on a small A value, 5×10^4 s^{-1}, for the *trans* isomer [100]. However, this was a typographical error and the correct value is 5×10^{14} s^{-1} [101].

Φ_{rx} is large in *cis*-$Cr(cyclam)(NH_3)_2^{3+}$ but negligible in the *trans* counterpart. This result points to $^4T_2$ as the seat of the delayed reaction.

The results of other caged complexes, $Cr(sar)^{3+}$ (sar = 3,6,10,13,16,19-hexaazabicyclo[6.6.6]icosane) and the diamino derivative $Cr(diamsar)^{3+}$ [102,103], support the thesis that trigonal twisting is necessary for good thermal quenching. The lifetime of $Cr(sar)^{3+}$ is

Table 1

Complex	Solvent	T range (K)	k_0 (s^{-1})	A (s^{-1})	E (kJ mol^{-1})	References
$Cr(NH_3)_6^{3+}$	DMF–$CHCl_3$	180–285	1.3×10^{4}		47	[96]
$Cr(NH_3)_6^{3+}$	DMF	253–288			45.2	[149]
$Cr(NH_3)_6^{3+}$	EGW			1.1×10^{12}	37.2	[87]
$Cr(NH_3)_6^{3+}$	DMSO–H_2O		1.3×10^{4}	1×10^{12}	46.9	[32]
$Cr(NH_3)_6^{3+}$	H_2O	273–294		1.1×10^{14}	41.8	[208]
$Cr(ND_3)_6^{3+}$	H_2O	273–294		5.8×10^{14}	52.3	[208]
$Cr(ND_3)_6^{3+}$	DMF–$CHCl_3$	180–285	2.9×10^{2}		48	[96]
$Cr(en)_3^{3+}$				1.2×10^{13}	40	[209]
$Cr(en)_3^{3+}$	DMF	253–288			46.9	[149]
$Cr(en)_3^{3+}$	H_2O	273–294		1.1×10^{13}	41.8	[208]
$Cr(en)_3^{3+}$			1.1×10^{4}	1.6×10^{14}	47.3	[1]
$Cr(en)_3^{3+}$	H_2O	286–318			40.8	[84]
$Cr(tn)_3^{3+}$			9.2×10^{3}	1.7×10^{12}	38.0	[1]
t-$Cr(cyclam)(NH_3)_2^{3+}$	H_2O	274–333	5.7×10^{3}	5×10^{14}	59	[100]
t-$Cr(cyclam)(NH_3)_2^{3+}$	H_2O	[a]		2.7×10^{15}	64	[210]
t-$Cr(cyclam)(NH_3)_2^{3+}$	DMF	[a]		3.3×10^{15}	69	[210]
t-$Cr(cyclam)(NH_3)_2^{3+}$	H_2O	283–334	5.7×10^{3}	6×10^{15}	65	[34]
c-$Cr(cyclam)(NH_3)_2^{3+}$	H_2O	281–320			43	[34]
c-$Cr(cyclam)(NH_3)_2^{3+}$	H_2O	274–313			36	[100]
c-$Cr(cyclam)(NH_3)_2^{3+}$	H_2O–MeOH	263–293		2.7×10^{12}	37	[211]
$Cr(cyclam)(en)^{3+}$	DMSO–H_2O		7.4×10^{3}	2×10^{13}	43.9	[32]
c-$Cr(cyclam)(NH_3)_2^{3+}$	H_2O–MeOH	283–323		$3\times0\times10^{12}$	41	[211]
c-$Cr(cyclam)(NH_3)_2^{3}$				2×10^{13}	44.3	[209]
$Cr([9]aneN_3)_2^{3+}$	DMSO–H_2O	250–295		6.3×10^{11}	42	[212]
		35–150			0.5	
D-$Cr([9]aneN_3)_2^{3+}$	DMSO–H_2O	250–295		5×10^{12}	47	[212]
$Cr(BCNE)^{3+}$				2.5×10^{11}	17.9	[209]
t-$tetb(NH_3)_2^{3+}$	DMSO–H_2O		5.4×10^{3}	8×10^{9}	31.4	[32]
Cr(TCTA) [b]				3.8×10^{14}	29.9	[209]
$Cr(sen)^{3+}$	DMSO–H_2O				29	[95]
	$Rh(sen)(ClO_4)_3$				33	[95]
$Cr(sep)^{3+}$	DMF	253–288			51.0	[149]
$Cr(diamsar)^{3+}$	CH_3CN	100–210			29	[103]
$Cr(NH_3)_5(CN)^{2+}$	H_2O	283–303		1.1×10^{13}	47	[213]
$Cr(NH_3)_5(CN)^{2+}$	DMSO	291–311		1.9×10^{14}	55	[213]
$Cr(NH_3)_5(CN)^{2+}$	DMF	284–308		1.4×10^{14}	53	[213]
$Cr(NH_3)_5(NCS)^{2+}$	DMSO–H_2O		1.11×10^{4}	3×10^{12}	33.9	[32]
$Cr(NH_3)_5(Cl)^{2+}$	DMSO–H_2O		2.4×10^{4}	2×10^{21}	54.4	[32]
$Cr(NH_3)_5(Cl)^{2+}$	$[Rh(NH_3)_5Cl]Cl_2$		2.3×10^{4}	1×10^{11}	28.9	[32]
$Cr(NH_3)_5F^{2+}$	DMSO–H_2O		2.0×10^{4}	6×10^{13}	30.1	[32]
$Cr(NH_3)_5(H_2O)^{3+}$	DMSO–H_2O		1.76×10^{4}	2×10^{13}	32.2	[32]
$Cr(NH_3)_5(H_2O)^{3+}$	EGW	162–212			33	[87]
$Cr(NH_3)_5(H_2O)^{3+}$	Glycerol–H_2O	200–244			50	[87]
$Cr(NH_3)_5(ONO)^{3+}$	DMSO–H_2O		1.6×10^{4}	8×10^{12}	26.8	[32]
$Cr([14]aneN_3S)(NH_3)_2^{3+}$	DMSO–H_2O		8.6×10^{3}	6×10^{12}	35.1	[32]
t-$Cr(cyclam)(CN)_2^{+}$	H_2O	Near ambient		2×10^{9}	27.5	[216]
t-$Cr(cyclam)(NH_3)(CN)^{2+}$	H_2O	Near ambient		1×10^{13}	47.0	[216]
t-$Cr(cyclam)(NCS)(CN)^{+}$	H_2O	Near ambient		2×10^{11}	38.1	[216]
t-$Cr(cyclam)(H_2O)(CN)^{2+}$	H_2O	Near ambient		6×10^{15}	54.9	[216]
t-$Cr(cyclam)(F)(CN)^{+}$	H_2O	Near ambient		6×10^{15}	46.8	[216]
t-$Cr(cyclam)Cl(CN)^{+}$	H_2O	Near ambient		5×10^{14}	45.5	[216]
t-$Cr(NH_3)_4(CN)_2^{+}$	H_2O	281–303		2.0×10^{9}	27.6	[213]
t-$Cr(NH_3)_4(CN)_2^{+}$	DMSO	291–311		3.5×10^{14}	55	[213]
c-$Cr(NH_3)_4(CN)_2^{+}$	H_2O	280–303		2.2×10^{9}	27	[213]
c-$Cr(NH_3)_4(CN)_2^{+}$	DMSO	291–311		3.2×10^{9}	30	[213]
c-$Cr(NH_3)_4(CN)_2^{+}$	DMF	280–307		9.8×10^{8}	25	[213]
t-$Cr(NH_3)_4(H_2O)(CN)^{2+}$	H_2O	279–303		5.8×10^{15}	55	[213]
t-Cr(D-cyclam)$(CN)_2^{+}$	H_2O	320–550			38	[215]
c-$Cr(tetb)(CN)_2^{+}$	H_2O	Near ambient			50	[99]
c-$Cr(tetb)(CN)_2^{+}$				4.2×10^{13}	45.4	[209]
t-$Cr(en)_2(NCS)_2^{+}$	H_2O	278–308			29.3	[84]
t-$Cr(en)_2(NCS)_2^{+}$	H_2O	273–294		7.2×10^{10}	31.8	[208]
t-$Cr(cyclam)Cl_2^{+}$	DMSO–H_2O		1.1×10^{4}	4×10^{19}	49.9	[32]

Table 1 (*Continued*)

Complex	Solvent	T range (K)	k_0 (s^{-1})	A (s^{-1})	E (kJ mol^{-1})	References
c-$Cr(cyclam)Cl_2^+$	DMSO–H_2O		1.9×10^4	1×10^{13}	27.2	[32]
c-$Cr(cyclam)Cl_2^+$				4×10^{12}	25.1	[209]
t-$Cr([15]aneN_4)Cl_2^+$	DMSO–H_2O		1.5×10^4	3×10^{22}	59.8	[32]
t-$Cr(cyclam)(NH_3)Cl^{2+}$	DMSO–H_2O		9.6×10^3	7×10^{13}	35.9	[32]
c-$Cr(cyclam)(NCS)_2^+$	DMSO–H_2O		1.04×10^4	7×10^{10}	31.4	[32]
t-$Cr(cyclam)(H_2O)_2^{3+}$	DMSO–H_2O		9.4×10^3	3×10^{13}	31.8	[32]
c-$Cr(tetb)(NCS)_2^+$				1×10^{12}	27.5	[209]
$Cr(NH_3)_3(NCS)_3$	EtOH	Fluid		1×10^{16}	36	[26]
$Cr[14]aneN_3S)Cl_2^+$	DMSO–H_2O		1.5×10^4	3×10^{23}	61.5	[32]
t-$Cr(NH_3)_2(NCS)_4^-$	H_2O	273–294		4.3×10^{15}	41.8	[208]
t-$Cr(NH_3)_2(NCS)_4^-$	Alcohol–H_2O	160–2	3.8×10^3	6.1×10^{14}	41.5	[1]
t-$Cr(NH_3)_2(NCS)_4^-$	EtOH	200–290		5×10^{14}	40	[26]
t-$Cr(NH_3)_2(NCS)_4^-$	Acetone	200–290		2×10^{15}	48	[26]
t-$Cr(NH_3)_2(NCS)_4^-$	Acetone			6.3×10^{14}	46	[93]
t-$Cr(NH_3)_2(NCS)_4^-$	PG	200–290		5×10^{16}	51	[26]
t-$Cr(NH_3)_2(NCS)_4^-$	H_2O	278–318			26.9	[84]
t-$Cr(NH_3)_2(NCS)_4^-$	Various	278–303		10^{15}–10^{17}	41–55	[90]
t-$Cr(NH_3)_2(NCS)_4^-$	Alcohol–H_2O	163–235			26	[217]
t-$Cr(NH_3)_2(NCS)_4^-$	Acetone–H_2O	220–295		3.8×10^{15}	49.3	[245]
$Cr(phen)(CN)_4^-$	DMSO–H_2O			5.8×10^{12}	33	[33]
$Cr(acac)_3$	$Al(acac)_3$	80–220		6.10^{12}	33.5	[255]
$Cr(acac)_3$	Alcohol–H_2O	135–195			25	[217]
$Cr(NCS)_6^{3-}$	Acetone–H_2O	235–295		5.2×10^{15}	49.7	[245]
$Cr(NCS)_6^{3-}$	EtOH	Fluid		7×10^{15}	44	[26]
$Cr(NCS)_6^{3-}$	Alcohol–H_2O	183–240			30	[217]
$Cr(NCS)_6^{3-}$	H_2O	280–317			33.5	[84]
$Cr(urea)_6^{3+}$	H_2O	270–310			0	[84]
$Cr(o\times)_3^{3-}$	H_2O	270–310			5.4	[84]
t-$Cr(py)_4F_2+$	H_2O	286–318			49.9	[84]
$Cr(CN)_6^{3-}$	Alcohol–H_2O		2.5×10^2	1.4×10^{11}	30.5	[33]
$Cr(CN)_6^{3-}$	CH_3CN	278–322		4.7×10^6	24	[106]
$Cr(CN)_6^{3-}$	EtOH	223–330		2.7×10^9	31	[106]
$Cr(CN)_6^{3-}$	Various			10^8–10^{12}	20–37	[106]
$Cr(CN)_6^{3-}$	DMF				33.5	[107]
$Cr(CN)_6^{3-}$	DMF			6×10^8	38	[106]
$Cr(CN)_6^{3-}$	Alcohol–H_2O	153–250			25	[217]
$Cr(bpy)_3^{3+}$				2×10^9	30.2	[33]
$Cr(bpy)_3^{3+}$	H_2O	273–294		3.6×10^9	29.2	[208]
$Cr(bpy)_3^{3+}$	DMSO–H_2O	185–294	200	9.7×10^9	30.0	[35]
$Cr(phen)_3^{3+}$				6×10^{10}	38.4	[209]
$Cr(tpy)_2^{3+}$				2×10^{17}	47.8	[209]
c-$Cr(phen)_2(NH_3)_2^{3+}$				3×10^{11}	34.7	[209]
$Cr(phen)(en)_2^{3+}$	DMSO–H_2O	170–265		2.8×10^{11}	30.2	[33]
$Cr(bpy)(en)_2^{3+}$	DMSO–H_2O	170–265		2.4×10^{11}	29.5	[33]
c-$Cr(bpy)_2(CN)_2^+$	DMSO–H_2O	150–250		1.0×10^{13}	33.6	[33]
c-$Cr(phen)_2(NCS)_2^+$	DMSO–H_2O	150–250		5.1×10^{11}	34.8	[33]
c-$Cr(bpy)_2(NCS)_2^+$	DMSO–H_2O	161–265		4.1×10^{11}	34.8	[33]

[a] High temperature value from two-exponential fit.
[b] TCTA = 1,4,7-tris(acetato) 1,4,7 triazacyclononane.

reduced from 65 μs at 77 K to <10 ns at 298 K [104]. The abrupt $k(T)$ increase in $Cr(diamsar)^{3+}$ does not appear to require solvent motion [103]. There was very little thermal quenching in another caged complex with the ligand *fac*-1,5,9,13,20-pentamethyl-3,7,11,15,18,22-hexaazabicyclo[7.7.7]tricosane [102]. The marked difference between these complexes was again attributed to larger trigonal twist in $Cr(sar)^{3+}$ and $Cr(diamsar)^{3+}$ compared with the other caged complex. $k_{nr}^{E}(T)$ was implicated as the source of the thermal decay pathway in $Cr(sar)^{3+}$, but the enhancement was ascribed to an increase in β rather than F in Eq. (19). The reduction in the $Cr(diamsar)^{3+}$ lifetime at 200 K corresponds to $E = 29$ kJ mol^{-1} and $A = 10^{13}$–10^{14} s^{-1}.

3.2.2. $Cr(N_4)XY$ and $Cr(NH_3)_5X$ complexes

Substitution of one or two nitrogen coordinating ligands in CrN_6 complexes by other ligands can increase the average ligand field (CN^-) or decrease it (halides and H_2O). Decreasing the ligand field would

reduce the $^4T_2$ energy and delocalization of *d* electrons onto CN^- and NCS^- decreases the ^2E energy. Several of the results for complexes in this group are associated with unrealistically high *A* values. No clear interpretation of the data for this group can be made.

Replacing an NH_3 ligand by Cl^- reduces the $^4T_2$–^2E gap. The concomitant reduction in *E* results in nonexponential decay in a rigid solvent when $k(T)$ is significant [94]. $k(T)$ for $Cr(NH_3)_6^{3+}$ in the same solvent begins in the fast solvent domain as evidenced by the exponential decay.

3.2.3. $Cr(CN)_6^{3-}$

This complex is of particular interest since the strong field CN^- ligand, coupled with a lowering of ^2E by delocalization ($\lambda_{em} = 810$ nm), leads to such a large $^4T_2$–^2E separation that k_{bisc} is negligible at ambient temperatures [105]. Consequently, the activation parameters should correspond to a pathway in which back-intersystem crossing can be ignored. The photoreaction is entirely prompt and is unaffected by ^2E relaxation as expected if k_{bisc} is negligible. Therefore, the thermal decay pathway is via $k_{nr}^E(T)$.

The decays are exponential in both rigid and fluid media [26], although there appear to be specific solvates with low energies [254]. The *E* values are very solvent dependent and range from 21 to 38 kJ mol^{-1} near r.t. [106]. In dimethylformamide (DMF) there is a poor fit in the absence of external quenchers ($E = 33.5$ kJ mol^{-1}) but a much better fit in the presence of 0.01 M ICN with $E = 38$ kJ mol^{-1} and $A = 5 \times 10^{10}$ [107]. This latter *E* is in concord with the earlier report [106]. Some of the variation in *E* and *A* may be due to fitting errors, but the sensitivity of the thermal decay to environment is evident.

When $Cr(CN)_6^{3-}$ is in an isostructural crystalline host, $k(T) \approx k_r(T)$ and the temperature dependence is quite small [88]. k_0 is also very small in the crystal, 8 s^{-1}. This compares with 240 s^{-1} in rigid alcohol–water at 77 K [7]. Sorbitol suppresses $k(T)$ completely at r.t. [26].

3.2.4. $Cr(urea)_6^{3+}$ and $Cr(H_2O)_6^{3+}$

These two complexes represent the extreme of a small $^4T_2$–^2E gap as evidenced by thermally induced fluorescence even at low temperatures [86,88]. In some crystals, but not all, the $Cr(urea)_6^{3+}$ decays are exponential [109,110]. Exponential decays are also observed in Cr^{3+}:$AlCl_3 \cdot 6D_2O$, where the complex is $Cr(D_2O)_6^{3+}$ and a weak thermally induced fluorescence is detectable [88]. The delayed fluorescence due to k_{bisc} is accompanied by marked nonexponentiality in glassy solutions of $Cr(urea)_6^{3+}$ [110]. The fluorescence and phosphorescence decay rates are different under these conditions. This difference, coupled with the nonexponential decays, demonstrates the sensitivity of k_{bisc} to environment.

3.2.5. $Cr(ox)_3^{3-}$ and amineoxalates

$Cr(ox)_3^{3-}$ is another complex with a small $^4T_2$–^2E gap in which $k(T)$ is large at 77 K. The decays, which are exponential in Cr^{3+}:$NaMgAl(ox)_3 \cdot 9H_2O$ at all temperatures, are nonexponential in a rigid matrix at 77 K [94]. The $^4T_2$–^2E gap increases progressively with replacement of ox^{2-} by NH_3. In rigid solutions, the temperature at which $k(T)$ becomes appreciable increases in the order $Cr(ox)_3^{3-} < Cr(ox)_2(NH_3)_2^- < Cr(ox)(NH_3)_4^+$ [94]. The $^4T_2$–^2E gap increases in the same order. In all three complexes increasing $k(T)$ is accompanied by increasing nonexponentiality in the slow solvent motion regime. These results again point to the importance of k_{bisc} as an important component of $k(T)$.

In contrast to $Cr(urea)_6^{3+}$, no fluorescence is detectable at any temperature in these complexes. This demonstrates that the absence of delayed fluorescence does not rule out back-intersystem crossing as an important process.

3.2.6. $Cr(polypyridine)_3^{3+}$ complexes

$Cr(bpy)_3^{3+}$ and $Cr(phen)_3^{3+}$ have large and nearly equal $^4T_2$–^2E gaps (> 70 kJ mol^{-1} [33]). The *E* values are about 30 kJ mol^{-1}, respectively, in several solvents. Back-transfer should not be possible in these complexes. The *A* values are somewhat small, suggesting that $k_{nr}^E(T)$ is the source of the thermal decay. The onset temperature for $k(T)$ varies with solvent [44]. The decays are exponential in rigid media.

Parenthetically, no emission was detected from $V(bpy)_3^{2+}$ and $V(phen)_3^{2+}$ in the 700–1100 nm range at 77 K [112]. The ^2E lifetime was determined by transient absorption to be ~ 1 μs at r.t.

3.3. Tetragonal complexes

There is a group of complexes in which large tetragonal fields lead to such a large $^2T_1$ splitting that one of the components ($^2E^Q$) is below ^2E and the emission is the broader $^2E^Q \Rightarrow {}^4T_2$ band that peaks at longer wave lengths [113–115]. The position of the $^2E^Q \Rightarrow {}^4A_2$ band is often solvent dependent—a redshift is induced when the rigid solvent is changed from hydrogen-bonding to non-hydrogen-bonding [83]. The emission maximum of *cis*-$Cr(phen)_2F_2^+$ in DMF–H_2O shifts from 730 to 810 nm as the water content is decreased. Hydrogen-bonding appears to increase the $^2E^Q$ energy. The tetragonal field also splits $^4T_2$, but there is no compelling evidence for back-transfer as the dominant thermal decay process.

The *trans*-$Cr(py)_4F_2^+$ and *trans*-$Cr(py)_4FBr^+$ $^2E^Q$ decays are slightly nonexponential in rigid media, but the

nonexponentiality is more marked in *cis*-$Cr(phen)_2F_2^+$ solutions [44]. In some cases, *cis*-$Cr(phen)_2F_2^+$ for example, there is a $^2E^Q-^2E$ level inversion induced by solvent motion, which apparently disrupts hydrogen-bonding. The spectral broadening and redshift occurs between 178 and 184 K in EGW.

The redshift induced by solvent motion is accompanied by an increased k_{relax} as expected from the energy gap law. In *trans*-$Cr(py)_4F_2^+$ and *trans*-$Cr(py)_4FBr^+$ there is a plateau in the lifetime–temperature plot that is analogous to that observed in Ru(II) polypyridine complexes (Section 4.2.1). This, coupled with the solvent motional induced redshift, suggests that at least part of the enhanced thermal decay is due to increased nonradiative decay that accompanies the lowering of $^2E^Q$.

3.4. Population of ^2E

Excitation is usually into the quartet manifold. The fraction of the excitation that is transferred to ^2E after absorption in the quartet manifold is [5]:

$$\Phi_D = \eta_{pisc} + (1-\eta_{pisc}-\eta_{pr})\eta_{isc} \equiv \eta'_b \quad (20)$$

where η_{pr} is the fraction of excitation that leads to prompt reaction. Unless $\eta_{bisc}=0$, η'_b is not the same as η_b, the fraction of the total reaction that is quenchable, since η_b includes contributions from multiple passes between $^4T_2$ and ^2E. η_b is also obtained by comparison of the slow and fast components of reaction by the pulsed conductivity method [116]. η_b can exceed Φ_D. Kirk [5] has summarized the estimates for Φ_D. With few exceptions, $\Phi_D \geq 0.7$. Inferences based on ^2E lifetimes are not affected by uncertainties in Φ_D. There has been a report that the quenchable $Cr(NH_3)_6^{3+}$ Φ_{rx} varies with the excitation wave length [117], which indicates η_{pisc} or η_{pr} also contributes at some wave lengths. However, the fraction of the conductivity changes that occur with the same lifetime as the ^2E decay is not only higher than the quenchable fraction but also the wave length dependence is smaller and in the opposite direction [116]. In these two studies, it was η_b that was computed and the lack of agreement indicates the difficulty in assessing intersystem crossing magnitudes.

Evidence has been presented for an unquenchable reaction in rigid glass solutions of $Cr(NH_3)(NCS)_4^-$ [92].

3.5. Mechanistic inferences

The extensive debate about the relative contributions to $k(T)$ underscores the difficulty of evaluating the pathways for the nearly universal thermal enhancement of excited state relaxation. Changes in excited state potential surfaces could enhance both k_{bisc} and $k_{nr}(T)$ The evidence provided by the E values collected in Table 1 is, at most, suggestive. Rough estimates of the $^4T_2-^2E$ gap from spectra, the effect of solvent motion on $k(T)$, and the extent of nonexponential decay lead to a model in which k_{bisc} is a dominant contribution to $k(T)$ in most cases. A definite exception to this generalization is $Cr(CN)_6^{3-}$ where the $^4T_2-^2E$ gap is too large for back-transfer. Back-transfer in $Cr(polypyridine)_3^{3+}$ complexes also seems improbable. The effect of solvent mobility on $k(T)$ in the two large gap complexes is different than in the other complexes. This suggests a different decay pathway when back-transfer is energetically prohibited.

4. d^6 complexes

4.1. Classification of emitting levels

In contrast to the d^3 complexes, where only MC states of Cr(III) are involved in the decay pathway, states of different orbital parentage, ^{3}MC, ^{3}MLCT, and ^{3}LC can participate in the excited state depopulation of d^6 complexes. A useful first step in unraveling the mechanism is the classification of the emitting state in terms of orbital parentage. Criteria for classifying the emitting state as ^{3}MC (d–d*), ^{3}MLCT (d–π*), or ^{3}LC (π–π*) were advanced many years ago [118] and have been very useful. They are not, however, sufficient for assignments in some Rh(III) and Ir(III) complexes [30]. These criteria include spectral shape and position, and the effect of ligand and solvent changes on the emission. The relative order of the three types of excited states is dependent on the metal ion and the ligands. ^{3}LC emission, exemplified by $Rh(phen)_3^{2+}$, is structured and resembles the free ligand emission, slightly redshifted. In contrast, ^{3}MC emission is unstructured and the energy depends upon the Dq values of the coordinated ligands. Cyclometallation of an azaaromatic ligand involves replacement of a coordinated nitrogen by a carbon atom. This change increases the ligand field strength markedly. ^{3}MC emission corresponds to $^3T_1 \Rightarrow {}^1A_1$ in octahedral symmetry and the broad band is the result of the geometry change that accompanies the promotion of a t_2 electron to an e orbital.

The position of the ^{3}MLCT level is sensitive to the difference between the ligand reduction potential and the metal oxidation potential [119]. The assignment of this level is problematical when configuration mixing with ^{3}LC or ^{3}MC levels is significant. The structure of a putative ^{3}MLCT emission can closely resemble a ^{3}LC band [121]. Zeeman splitting patterns obtained under resonant line narrowed conditions have provided a useful criterion for distinguishing ^{3}MLCT from ^{3}LC emission [30,120]. ^{3}MLCT emission spectra in fluids are invariably structureless. Since the ^{3}MLCT spectra exhibit rigidochromic redshifts, the emitting level can be

^{3}LC or ^{3}MC in a rigid glass and ^{3}MLCT in a fluid. Consequently, the level ordering at low and ambient temperatures may differ.

Macroscopic rigidity does not necessarily imply lack of environmental motion on the microscopic level. Ru(II) and Os(II) complexes with polypyridine ligands in a rigid matrix exhibit thermally induced red shifts [108,122].

The lifetime has been suggested as diagnostic for the assignment of the emission [118]. While ^{3}LC lifetimes at 77 K are usually ≥ 100 μs and ^{3}MLCT and ^{3}MC lifetimes are shorter, this parameter is not always a reliable guide for characterizing the emitting level. The magnitude of the radiative rate may be a more useful quantity [123], but even here mixing between states can cloud the picture.

Each level is split into a number of sublevels. Under some conditions, particularly ^{3}MLCT emitters at low temperatures, the differential decay rates of the sublevels leads to significant thermal changes in k_{relax}. At higher temperatures, the sublevel splittings can be ignored and the manifold treated as a single level, since the relative populations will not change appreciably with temperature.

Although the orbital parentage classification is less valid when excited states belonging to different categories are proximate, it has proven useful in systematizing a large body of results. There has been some question about the validity of the spin designations [124,234]. In this review no harm will follow from labeling the states as singlets and triplets.

Emission in Ru(II) and Os(II) complexes is usually limited to complexes with at least one azaaromatic ligand, but ^{3}MC emission is obtained in Rh(III) complexes without azaaromatic ligands. The lowest energy excited level in most Co(III) amines is a MC quintet state that provides a facile nonradiative relaxation pathway and explains the absence of emission [[126], Endicott in [127]]. A conspicuous exception is $Co(CN)_6^{3-}$, where the strong field ligand depresses $^3T_1$ below $^5T_2$. That no emission has been reported from Fe(II) complexes can also be ascribed to low-lying $^5T_2$ levels.

4.2. Thermal relaxation

4.2.1. Ru(II) complexes

The complexes of Ru(II) have been the subject of more photochemical and photophysical studies than any other d^6 ion. The lifetimes and emission quantum yields at r.t. and 77 K of more than 200 Ru(II) complexes have been tabulated [4]. The less extensive literature on the thermal dependence of the decay rates over a wide temperature range has been reviewed [128] but a more complete summary of the extant results is collected in Table 2.

The emitting state in Ru(II) complexes is usually ^{3}MLCT in character. $Ru(i\text{-biq})_3^{2+}$ is an exception to this generalization. The assignment of the emission in this complex as $^3LC \Rightarrow {}^1A_1$ is based on the similarity between the emission spectra of the complex and the free ligand and the relatively long emission lifetime [128,129]. Cyclometallation also leads to ^{3}LC emission [130]. The ^{3}MLCT energy is a linear function of the difference between the metal oxidation potential and the reduction potential of the most easily reduced ligand [119]. ^{3}MC emission is rare in Ru(II) complexes and the ^{3}MC energy can only be estimated indirectly from kinetic data. The approach used in assigning the emitting levels in $Ru(NN)_3^{2+}$ and *cis*-$Ru(NN)_2Cl_2$ (NN = bpy, biq, *i*-biq, DMCH) has been detailed [129,131]. All three types of emitting levels were identified, but there is uncertainty in the assignment of the *cis*-$Ru(i\text{-biq})_2Cl_2$ emission as a superposition of ^{3}MLCT and ^{3}MC.

The main points to be addressed are the reliability of the thermal activation parameters and the use of these parameters for the assessment of the relaxation pathway. Secondary issues are the effect of environmental rigidity on k_{relax} and the connection between the ^{3}MLCT decay rate, photochemistry and the population of ^{3}MC.

4.2.1.1. Ru(bpy)$_3^{2+}$. The spectroscopy of $Ru(bpy)_3^{2+}$ has been critically reviewed [133] and this complex provides a basis for describing Ru(II) complexes in general. In this model, thermal equilibrium is established among the lowest three ^{3}MLCT sublevels and the k_{relax} variation below 77 K is due to the changing population of these closely spaced levels [11]. The validity of the equilibrium hypothesis in $Ru(bpy)_3^{2+}$ and the precise values of the energy separations within the ^{3}MLCT manifold has been questioned [133] but it has been demonstrated that equilibration is achieved down to 1.4 K at low laser powers, although some departure from thermal equilibrium obtains at high excitation energies below 20 K [134]. By combining lifetime and quantum yield data it was possible to extract the radiative and non-radiative rates for each of the three ^{3}MLCT sublevels in $Ru(bpy)_3^{2+}$ dissolved in polymethylmethacralate (PMM) [11]. Assuming thermalization, a good fit to

$$k_{relax} = \frac{5.46 \times 10.64 \times \exp\left(-\frac{10.1}{k_B T}\right) + 1.47 \times 10^6 \exp\left(-\frac{61.2}{k_B T}\right)}{1 + 2\exp\left(-\frac{10.1}{k_B T}\right) + \exp\left(-\frac{61.2}{k_B T}\right)} \quad (21)$$

was obtained. The energies in Eq. (21) are in cm^{-1} and the preexponential factors in s^{-1}. Since the relaxation

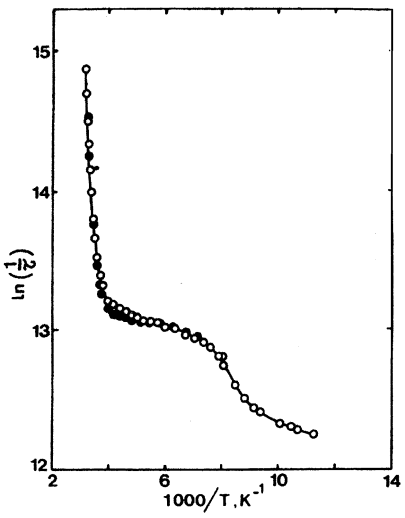

Fig. 2. Temperature dependence of emission lifetime (○) and relative emission intensity (●) for $Ru(bpy)_3^{2+}$ in propionitrile–butyronitrile (4:5 v/v). From reference [46] with permission from the American Chemical Society.

rates of the individual levels increase with energy, k_{relax} decreases markedly with temperature below 77 K, but more slowly at higher temperatures as the level populations become nearly constant. The emission quantum yield and lifetime do not change with temperature in a parallel fashion, as is usually the case, because the radiative rate increases in the higher energy ^{3}MLCT components more than the non-radiative rate. Several substituted $Ru(bpy)_3^{2+}$ complexes were also successfully analyzed by fitting to an analog of Eq. (21) [11].

Above 77 K, the equilibrium limit is replaced by the steady state limit corresponding to Eq. (14). With few exceptions [135], the transition between rigid and fluid solvents is accompanied by an abrupt change in lifetime, followed by a plateau where the activation energy is small, and a high temperature range with a large E_1 as shown in Fig. 2 [137]. The transition temperature interval is usually 20–30 K, solvent dependent and associated with a rigidochromic shift of the ^{3}MLCT emission to longer wave lengths. The correlation of the spectral and lifetime changes in the region of the rigid to fluid transition implicates solvent motion as the source of the abrupt increase in k_{relax}. In order to treat the thermal variation of k_{relax} in solvents where the temperature range spans the change from rigid (slow solvent motion) to fluid (fast solvent motion) Eq. (14) must be modified. Eq. (22) was introduced to allow for solvent motion changes [136].

$$k_0 = k'_0 + B/\{1 + \exp[C(1/T - 1/T_g)]\} \quad (22)$$

k'_0 is temperature independent and the abrupt change in the transition region is fitted by the second term in Eq. (22). This latter term was justified by a specific model for the effect of solvent motion on k_{relax} [51,136]. However, it could as well describe the k_{relax} increase induced by the lowering of the ^{3}MLCT–$^1A_1$ energy gap that is evidenced by the spectral shift. In any event Eq. (22) can be viewed as an empirical tool for extracting A_1, E_1, A_2, and E_2, over a temperature range that includes the rigid to fluid transition. The adequacy of this approach is validated by the results for $Ru(bpy)_3^{2+}$ in EM where the E_1 and A_1 parameters are nearly the same in the 84–330 K and the fluid (>140 K) ranges [137].

If the 'high temperature' domain is reached in the slow solvent motion limit, no plateau is observed. A comparison of the behavior of $Ru(biq)_3^{2+}$ in two solvents demonstrates this point; the plateau that obtains in PB is absent in EM [137].

Most of the results in Table 2 were obtained by fitting the data in a temperature range where the solvent was fluid and using Eq. (15) with one or two terms.

The extensive $Ru(bpy)_3^{2+}$ results permit evaluation of the reliability of the published parameters extracted by least-squares fitting. With one exception, E_1 obtained by single exponential fitting of the $Ru(bpy)_3^{2+}$ k_{relax} in a fluid solvent range from 3100 to 4040 cm^{-1} with $A_1 = 10^{13}$–10^{14} s^{-1}. E_1 is a measure of the energy necessary to reach the crossing between the ^{3}MC and ^{3}MLCT potential surfaces.

It is clear from Eq. (21) that a fit at low temperatures will yield an activation energy below 100 cm^{-1}. The E_1 and E_2 values greater than 100 cm^{-1} in Table 2 are not due to thermalization in the three lowest ^{3}MLCT levels, but result from population of higher levels. The ^{1}MLCT level is some 5000 cm^{-1} above ^{3}MLCT in $Ru(bpy)_3^{2+}$ [133] and other thermal decay pathways must be involved. These include fourth charge-transfer ($^3MLCT_{4th}$) and ^{3}MC levels.

Small activation energies (<1000 cm^{-1}) that are associated with small A_1 (10^6–10^9 s^{-1}) have been ascribed to relaxation through $^3MLCT_{4th}$ [138]. This level has been identified in the absorption spectrum of $Ru(bpy)_3(ClO_4)_2$ at 800 cm^{-1} above the emitting levels [134]. E_1 in pure crystals of $Ru(bpy)_3(PF_6)_2$ is larger than the solution values and the ^{3}MC level is only accessible above 300 K [43]. A rigid environment does not necessarily increase E_1 since the activation energy in $Ru(bpy)_3Cl_2{\cdot}6H_2O$ is only 3300 cm^{-1} even at high temperatures.

When $Ru(bpy)_3^{2+}$ is embedded in Zeolite and the decays recorded below 300 K, both E_1 and A_1 are drastically reduced. A similar reduction of the activation parameters occurs when other complexes are embedded in Zeolite. The small activation parameters point to decay via $^3MLCT_{4th}$ as the dominant thermal relaxation process in the temperature range 195–300 K [139]. This indicates that ^{3}MC cannot contribute to the thermal decay before $^3MLCT_{4th}$ quenches the emission. In PMM and boric acid the r.t. lifetime is greatly

Table 2

Complex	Solvent	T range (K)	k_0 (s^{-1})	A_1 (s^{-1})	E_1 (cm^{-1})	A_2 (s^{-1})	E_2 (cm^{-1})	References
$Ru(bpy)_3^{2+}$	EM	140–240	3.9×10^5	1.9×10^{14}	3859			[152]
$Ru(bpy)_3^{2+}$	CH_2Cl_2	200–296	4.1×10^5	4.5×10^{13}	3560			[39]
$Ru(bpy)_3^{2+}$	CH_2Cl_2	220–298	3.8×10^5	0.3×10^{13}	3068			[153]
$Ru(bpy)_3^{2+}$	EM	84–330	3.2×10^5	1.4×10^{14}	3950	4.6×10^5	84	[137]
$Ru(bpy)_3^{2+}$	EM	150–330	2.2×10^5	2.0×10^{14}	4040	5.0×10^5	69	[137]
$Ru(bpy)_3^{2+}$	PB	84–330	2.4×10^5	1.3×10^{14}	3960	5.6×10^5	90	[46]
$Ru(bpy)_3^{2+}$	PC	210–295	0.61×10^6	0.4×10^{13}	3275			[153]
$Ru(bpy)_3^{2+}$	CA	77–298	0.74×10^6	1.73×10^7	803	5.00×10^5	54	[1]
$Ru(bpy)_3^{2+}$	EM	Fluid		5.4×10^{12}	3100			[218]
$Ru(bpy)_3^{2+}$	Zeolite	195–300	3.8×10^5	1.1×10^8	890			[139]
$[Ru(bpy)_3](PF_6)_2$		350–480	4.3×10^6	7.6×10^{13}	5200			[43]
$[Ru(bpy)_3]Cl_2\cdot6H_2O$		>360	5.3×10^6	3.1×10^{12}	3300		80	[43]
$Ru(phen)_3^{2+}$	CH_2Cl_2	260–290	1.4×10^5	3.1×10^{13}	3180			[39]
$Ru(bpm)_3^{2+}$	PC	210–322	2.2×10^6	6.4×10^{13}	375			[154]
$Ru(mmb)_3^{2+}$	Zeolite	200–300	4.3×10^5	2.9×10^7	533			[139]
$Ru(bpz)_3^{2+}$	Zeolite	200–300	4.1×10^5	1.1×10^7	765			[139]
$Ru(biq)_3^{2+}$	PB	?84–250	4.5×10^5	1.8×10^{13}	2700			[137]
$[Ru(biq)_3](ClO_4)_2$		77–480	4.2×10^5	1×10^{13}	3100			[143]
$Ru(i\text{-}biq)_3^{2+}$	PB	84–330	1.0×10^4	1.0×10^{13}	2580			[46]
$Ru(decb)_3^{2+}$	CH_2Cl_2	220–298	0.33×10^6	3×10^7	1177			[153]
$Ru(dmb)_3^{2+}$	CH_2Cl_2	220–298	0.53×10^6	0.3×10^{12}	2741			[153]
$Ru(bpz)_3^{2+}$	PC	243–330	3.42×10^5	1.4×10^{14}	3902			[31]
$Ru(bpz)_3^{2+}$	PC	210–295	3.3×10^5	8×10^{12}	3325			[154]
$Ru(bpz)_3^{2+}$	Zeolite		4.1×10^5	1.1×10^5	765			[139]
$Ru(hat)_3^{2+}$	CH_3CN	230–330	2.3×10^4	2.1×10^{13}	3900	1.0×10^7	1030	[219]
$Ru(BL)_3^{2+}$	EM	150–298	2.45×10^6	2×10^9	1128			[144]
$Ru(pypm)_3^{2+}$	EM	160–295	1.17×10^6	5×10^{13}	3340			[147]
$Ru(4,4'\text{-}dpb)_3^{2+}$	PB	90–330	3.8×10^5	1.0×10^{14}	4700	8.7×10^5	300	[221]
$Ru(tpy)_2^{2+}$	EM	77–135	1.2×10^5	1.9×10^{13}	1500			[140]
$Ru(tpy)_2^{2+}$	PMM		1.1×10^5	2.4×10^6	23			[142]
$Ru(tpy)_2^{2+}$	Zeolite	220–290	1.5×10^5	9.3×10^{11}	2681	3.9×10^8	929	[222]
$[Ru(tpy)_2](PF_6)_2$		77–480	1.5×10^5	1.1×10^{12}	2000			[143]
$[Ru(tpy)_2](ClO_4)_2$		77–480	2×10^5	2×10^{11}	1100			[143]
$Ru(tsite)_2^{2+}$	EM	80–250	1.1×10^5	1.6×10^{13}	2300	2.4×10^5	110	[140]
$Ru(tpy\text{-}SO_2Me)_2^{2+}$	BN	250–ambient		1.3×10^{13}	2600			[135]
$Ru(4,4'\text{-}dpt)_2^{2+}$	EM	110–220	1.1×10^5	3.0×10^{13}	2200	2.3×10^6	360	[140]
$Ru(tpy)(4\text{-}etpy)_3^{2+}$	EM		7.4×10^5	0.5×10^{13}	2720			[141]
$Ru(tpy)(bpy)(NCCH_3)^{2+}$	PEN		1.7×10^5	2.1×10^{14}	1560			[142]
$Ru(tpy)(bpy)(NCCH_3)^{2+}$	PMM		1.2×10^5	3.1×10^6	160			[142]
$[Ru(tpy)(bpy)(NCCH_3)](PF_6)_2$			1.5×10^5	1.3×10^6	1200			[142]
$Ru(bpy)_2(py)_2^{2+}$	EM	140–240	4.2×10^5	2.3×10^{14}	2758			[152]
$Ru(bpy)_2(bpz)^{2+}$	PC	210–345	2.1×10^6	3×10^7	800			[154]
$Ru(bpy)_2(bpz)^{2+}$	Zeolite	200–300	5.4×10^5	19×10^7	894			[139]
$Ru(bpy)_2(bpm)^{2+}$	PC	210–345	1.2×10^7	1×10^7	400			[154]
$Ru(bpy)_2(NMI)_2^{2+}$	CH_2Cl_2	260–290	2.5×10^6	1.5×10^{13}	3500			[39]
$Ru(bpy)_2(AEP)^{2+}$	CH_2Cl_2	260–290	9.1×10^5	4.5×10^{13}	3240			[39]
$Ru(bpy)_2(py)_2^{2+}$	CH_2Cl_2	260–290	8.2×10^5	1.7×10^{13}	3410			[39]
$Ru(bpy)_2(phen)^{2+}$	CH_2Cl_2	260–290	3.7×10^5	6.9×10^{13}	3580			[39]
$Ru(bpy)_2(biq)^{2+}$	EM	84–330	1.4×10^6	2.0×10^7	420			[137]
$Ru(bpy)_2(biq)^{2+}$	PB	84–250	1.6×10^6	8.0×10^7	770			[52]
$Ru(bpy)_2(biq)(ClO_4)_2\cdot2H_2O$		77–480		3×10^{14}	5500	5.0×10^7	750	[143]
$Ru(bpy)_2(biq)(ClO_4)_2$		77–480		1.6×10^{12}	3600	8.0×10^4	300	[143]
$Ru(bpy)_2(biq)(PF_6)_2\cdot2H_2O$		77–480	1.5×10^6	6×10^{13}	4800	1.6×10^7	520	[143]
$Ru(bpy)_2(i\text{–}biq)^{2+}$	PB	84–330	3.1×10^5	4.8×10^{13}	3850	4.8×10^5	65	[46]
$Ru(bpy)_2(DMCH)^{2+}$	PB	84–250	1.2×10^6	2.6×10^7	630			[52]
$Ru(bpy)_2(4,4'\text{-}dpb)^{2+}$	PB	90–330	3.7×10^5	1.5×10^{14}	4100	6.7×10^5	350	[221]
$Ru(bpy)_2(pic)^{+}$	EM	140–343		1.3×10^{12}	2700			[223]
$Ru(bpy)_2(pyd)_2^{2+}$	CH_2Cl_2	260–290	3.4×10^5	1.5×10^{14}	2710			[39]
$Ru(bpy)_2(BL)^{2+}$	EM	150–298	5.41×10^5	2×10^9	789			[144]
$Ru(bpy)_2(dhab)^{2+}$	H_2O–HCl	283–363			310			[224]

Table 2 (*Continued*)

Complex	Solvent	T range (K)	k_0 (s^{-1})	A_1 (s^{-1})	E_1 (cm^{-1})	A_2 (s^{-1})	E_2 (cm^{-1})	References
$Ru(bpy)_2(dhab)^{2+}$	D_2O–DCl	283–363			630			[224]
$Ru(bpy)_2(dcb)^{2+}$	H_2O	283–363		1×10^{13}	4230			[224]
$Ru(bpy)_2(CO)H^{+}$	EM	145–300	6.78×10^{5}	1.05×10^{14}	1870			[225]
$Ru(bpy)_2(CO)D^{+}$	EM	145–300	1.35×10^{5}	1.14×10^{13}	1665			[225]
$Ru(bpy)_2(dmb)^{2+}$	Zeolite	200–300	4.3×10^{5}	6.8×10^{7}	777			[139]
$Ru(bpy)_2(diaz)^{2+}$	EM	140–250	3.1×10^{5}	8.5×10^{14}	2271			[152]
$Ru(bpy)_2(diaz)^{2+}$	Zeolite	208–300	1.8×10^{5}	0.8×10^{12}	4008	36.4×10^{7}	94	[145]
$Ru(bpy)_2(diaz)^{2+}$	Zeolite	208–300	4.2×10^{5}			63.2×10^{7}	1128	[145]
$Ru(bpy)_2(bpt)^{+}$	PB	77–250	3.5×10^{5}	4.0×10^{6}	260			[146]
$Ru(bpy)_2(bpt)^{+}$	PB	250–298		6.5×10^{7}	660			[146]
$Ru(bpy)_2(CN)_2$	PB	>140 and <140	2.8×10^{5}	$\times10^{10}$	2400	2.6×10^{7}	450	[136]
$Ru(bpy)_2(pypz)^{2+}$	PC	238–345	1.01×10^{5}	$.95\times10^{7}$	764			[226]
$Ru(bpy)_2(pypz)^{2+}$	Zeolite	200–333	8.21×10^{5}	6.04×10^{7}	703			[226]
$Ru(bpy)_2(hat)^{2+}$	CH_3CN	230–330	$133\times^{5}$	0.16×10^{12}	1685			[219]
$Ru(bpy)_2(pypm)^{2+}$	EM	160–295	1.18×10^{6}	2.2×10^{7}	550			[147]
$Ru(bpy)_2(NPP)^{2+}$	EM	120–142	1.2×10^{6}	2.6×10^{11}	956			[151]
$Ru(bpy)(bpm)(bpz)^{2+}$	PC	210–345	1.1×10^{6}	2.8×10^{8}	1415			[154]
$Ru(bpy)(BL)_2^{2+}$	EM	150–298	1.76×10^{6}	4×10^{9}	1417			[144]
$Ru(bpy)(bpm)_2^{2+}$	PC	210–295	5.1×10^{6}	3.2×10^{13}	3800			[154]
$Ru(bpy)(pypm)_2^{2+}$	EM	160–295	1.70×10^{6}	1.3×10^{7}	483			[147]
$Ru(bpy)(biq)_2^{2+}$	PB	84–250	6.4×10^{5}	3.0×10^{7}	300			[52]
$Ru(bpy)(i\text{-}biq)_2^{2+}$	PB	84–330	2.9×10^{5}	4.3×10^{13}	3890	7.8×10^{5}	110	[46]
$Ru(bpy)(bpz)(py)_2^{2+}$	EM	160–295	2.3×10^{6}	9×10^{6}	428			[147]
$Ru(bpy)(DMCH)_2^{2+}$	PB	84–250	6.8×10^{5}	1.2×10^{6}	190			[52]
$Ru(bpy)(hat)_2^{2+}$	CH_3CN	230–330	40×10^{5}	0.11×10^{12}	2728			[219]
$Ru(bpy)(hat)_2^{2+}$	CH_3CN	230–330	40×10^{5}	8.4×10^{12}	3700	4.4×10^{12}	1260	[219]
$Ru(bpy)(4,4'\text{-}dpb)_2^{2+}$	PB	90–330	4.3×10^{5}	1.2×10^{14}	4300	1.2×10^{6}	480	[221]
$Ru(bpy)(tap)(hat)^{2+}$	CH_3CN		230–330	46×10^{5}	0.97×10^{12}	3245		[219]
$Ru(bpy)(bpz)_2^{2+}$	PC	210–345	7.4×10^{5}	4×10^{9}	2100			[154]
$Ru(bpy)(bpz)_2^{2+}$	PC	243–330	7.39×10^{5}	1.3×10^{9}	1859			[31]
$Ru(bpy)(bpz)_2^{2+}$	PC	243–373	6.4×10^{5}	9×10^{13}	4632	8×10^{6}	736	[31]
$Ru(bpm)_2(py)_2^{2+}$	EM	160–295	8.7×10^{6}	3×10^{17}	4776			[147]
$Ru(bpm)(bpz)_2^{2+}$	PC	210–345	4.75×10^{5}	8×10^{13}	3917			[154]
$Ru(bpm)_2(bpz)^{2+}$	PC	210–345	7.4×10^{5}	3.5×10^{13}	3850			[154]
$Ru(dmb)_2(py)_2^{2+}$	EM	160–295	7.1×10^{5}	4×10^{15}	3244			[147]
$Ru(bpz)_2(py)_2^{2+}$	EM	160–295	1.06×10^{6}	5×10^{14}	4212			[147]
$Ru(biq)_2(CN)_2$	PB	<140 and >140		2.6×10^{6}	620			[66]
$Ru(i\text{-}biq)_2(CN)_2$	PB	167–310		8.0×10^{13}	3800	4.3×10^{7}	640	[66]
$Ru(dmb)_2(decb)^{2+}$	CH_2Cl_2	220–298	0.65×10^{6}	4×10^{6}	447			[153]
$Ru(dmb)(decb)_2^{2+}$	CH_2Cl_2	220–298	0.41×10^{6}	5×10^{6}	612			[153]
$Ru(bpz)_2(dmb)^{2+}$	PC	243–330	9.1×10^{5}	1.9×10^{8}	1426			[31]
$Ru(bpz)_2(mmb)^{2+}$	PC	243–330	7.76×10^{5}	3.0×10^{8}	1521			[31]
$Ru(bpz)_2(mmb)^{2+}$	PC	243–373	6.7×10^{5}	9.0×10^{13}	4720	8×10^{6}	706	[31]
$Ru(bpz)_2(diaz)^{2+}$	PC	243–283	5.2×10^{5}	1.94×10^{15}	3627			[31]
$Ru(tpm)(4,4'X\text{-}bpy)py^{2+}$	EM							[228]
$X=C_6H_5$		130–280	0.95×10^{6}	3.3×10^{15}	4030			
$X=H$		130–250	1.3×10^{6}	0.13×10^{15}	3000			
$X=CH_3$		130–235	1.22×10^{6}	1.8×10^{15}	3200			
$X=NH_3$		130–175	0.77×10^{6}	1.1×10^{16}	2450			
$Ru(phen)_2(hat)^{2+}$	CH_3CN	230–330	100×10^{5}	4×10^{8}	1020			[219]
$Ru(tap)(hat)_2^{2+}$	CH_3CN	230–330	28×10^{5}	48×10^{12}	3127			[219]
$Ru(tap)(hat)_2^{2+}$	CH_3CN	230–330	26×10^{5}	93×10^{12}	3240	2.9×10^{12}	1000	[219]
$Ru(tap)_2(hat)^{2+}$	CH_3CN	230–330	23×10^{5}	122×10^{12}	3333			[219]
$Ru(tap)_2(hat)^{2+}$	CH_3CN	230–330	22×10^{5}	340×10^{12}	3490	3.1×10^{12}	1000	[219]
$Ru(biq)_2(1Meptr)^{2+}$	EM	150–300	1.1×10^{6}	5.0×10^{14}	1930			[229]
$Ru(biq)_2(H3Meptr)^{2+}$	EM	150–300	1.2×10^{6}	6.0×10^{11}	1230			[229]
$Ru(biq)_2(3Meptr)^{+}$	EM	150–300	2.1×10^{6}	1.6×10^{9}	340			[229]

increased, the decay is nonexponential and the photoreaction is suppressed [12,27]. These results underscore the sensitivity of the decay pathway to the environment and the temperature range explored.

4.2.1.2. Other complexes. As indicated above, the $Ru(bpy)_3^{2+}$ E_1 is nearly the same in both one- and two-exponential fits over a wide temperature range. There are few systems where this kind of comparison can be made, but the $Ru(bpy)(bpz)_2^{2+}$ and $Ru(bpz)_2(mmb)^{2+}$ results demonstrate that the two fitting models can yield very different results [31]. The single-exponential fits are definitely poorer for these complexes than those obtained by including two-exponential terms. The temperature range was extended from 330 to 373 K in the two-exponential fit. The single-exponential fits reflect an average of contributions from ^{3}MC and $^3MLCT_{4th}$ to the decay pathway. A priori, the two-exponential fits should be more reliable and the parameters, $E_1 \approx 4700\ cm^{-1}$ and $E_2 \approx 700\ cm^{-1}$ suggest two parallel decay pathways. The large E_1 requires higher temperatures in order to populate ^{3}MC.

In a good two-exponential fit, E_1 should correspond to the ^3MLCT–^{3}MC crossover. An E_2 value exceeding 100 cm^{-1} would reflect the ^3MLCT–$^3MLCT_{4th}$ separation.

CN^- is a high field ligand that should raise ^{3}MC and only a small activation energy of 620 cm^{-1} was extracted in the single-exponential fit of the $Ru(biq)_2(CN)_2$ decay.

The behavior of $Ru(tpy)_2^{2+}$ and the derivatives, $Ru(t\text{-}site)_2^{2+}$ and $Ru(4,4'\text{-}dpt)_2^{2+}$, differ markedly from that of $Ru(bpy)_3^{2+}$. The sharp break associated with the rigid-fluid transition in most ^{3}MLCT emitters is absent [140,141]. Furthermore, although A_1 is $10^{13}\ s^{-1}$, E_1 is only 1500–2300 cm^{-1} [135,140]. The small E_1 would be consistent with a lowering of the ^{3}MC energy produced by distortion from near octahedral geometry [142]. The large A_1 value indicates that ^{3}MC is the principle relaxation pathway.

The effect of the lattice on the activation energy is seen in a comparison of the $[Ru(tpy)_2](PF_6)_2$ and $[Ru(tpy)_2](ClO_4)_2$ results [143]. Changing the PF_6^- anion to ClO_4^- reduces E_1 from 2000 to 1100 cm^{-1}. A similar anion effect is obtained in $[Ru(bpy)_2biq](PF_6)_2{\cdot}2H_2O$ and $[Ru(bpy)_2biq](ClO4)_2{\cdot}2H_2O$ crystals.

A single-exponential model of the $Ru(bpy)(BL)_2^{2+}$ k_{relax} gives a good visual fit with $E_1 = 1417\ cm^{-1}$ [144]. However, $A_1 = 4 \times 10^9\ s^{-1}$ is indicative of an average of two processes.

The qualitative effect of rigidity on $Ru(bpy)_3^{2+}$ is also seen in other complexes. In general, $k(T)$ decreases at ambient temperatures. Activation parameters for a number of complexes in solution and in Zeolite are included in Table 2. Except for $Ru(tpy)_2^{2+}$, single-exponential fits lead to much smaller E_1 and A_1 values in Zeolite than in a fluid, as discussed in Section 4.2.1.1. When a double-exponential fit is used, both relaxation pathways are revealed. The ^{3}MC energy in $Ru(bpy)_2(diaz)^{2+}$ embedded in Zeolite, obtained by a double-exponential fit, is not exceptionally large [145]. The results of the single- and double-exponential fits over the same temperature range again demonstrates the dependence of the interpretation on the fitting model employed.

$Ru(bpy)_2(bpt)^+$ exhibits anomalous behavior [146]. There are two temperature regions where a redshift is observed. The lower temperature shift is associated with solvent motion, but the redshift at 160 K definitely occurs after solvent motion is fast. The spectral shift anomaly is reflected in the lifetime behavior and there are two different activation energies that are both small. No explanation for this phenomenon has been advanced.

In an enthalpy–entropy correlation [231] of activation parameters $\ln A_1$ is assumed to be a function of E_1 for a series of complexes in the same solvent [147] or for the same complex in different solvents [90,148]. Although, a linear relation is taken to indicate that the reaction mechanism, in one case [147] Ru(II) complexes with small and large E_1 fall on a line in a Barclay–Butler graph. Presumably, there is not a common relaxation pathway for the entire group of complexes. This demonstrates that a linear Barclay–Butler plot is not a reliable criterion for a common mechanism.

$Ru(bpy)_2(NPP)^+$ is a complex with a cyclometallated ligand. The emission has been assigned as $^3MLCT \Rightarrow {}^1A_1$ localized in the bpy ligand. Replacement of a bpy by NPP decreases the ^{3}MLCT energy in the bpy emitting ligand and increases the ^{3}MC energy. The result is to block population of ^{3}MC and $E_1 = 956\ cm^{-1}$ [151]. The absence of thermally activated photochemistry is consistent with failure to populate ^{3}MC. No rigidochromic effect is observed in a temperature range where the solvent viscosity changes drastically.

4.2.1.3. $RuA_nB_{3-n}^{2+}$ complexes. In Table 3 are series of complexes where the A and B ligands are azaaromatics. When A = bpy and B = *i*-biq, the presence of a single bpy is sufficient to ensure localization in that ligand as evidenced by the near constancy of λ_{em} and E_1 for $n = 1$–3. The π–π^* emission in $Ru(i\text{-}biq)_3^{2+}$ is higher in energy.

The emission energies of $Ru(bpy)_3^{2+}$ and $Ru(pypm)_3^{2+}$ are the same and the activation parameters are consistent with relaxation via ^{3}MC. In contrast, in the mixed ligand complexes the emission energy is somewhat reduced and the activation parameters point to $^3MLCT_{4th}$ as the principal relaxation contribution. If this interpretation is correct, the ^3MC–^{3}MLCT energy

Table 3

n	λ_{em} (nm)		E_1 (cm^{-1})	Φ_{rx}	η_{bc}	References
$Ru(bpy)_n(i\text{-biq})_{3-n}^{2+}$						[46]
	84 K	293 K				
3	583	608	3960		0.73	
2	586	610	3850		0.57	
1	586	615	3890		0.51	
0	540	543	2580 [a]			
$Ru(dmb)_n(decb)_{3-n}^{2+}$						[153]
	77 K	298 K				
3	593	618	2741	0.005	0.50	
2	642	696	447	$<10^{-3}$	0.047	
1	632	657	612	$<10^{-3}$	0.42	
0	607	629	1150	0.012	0.26	
$Ru(bpy)_n(bpm)_{3-n}^{2+}$						[154]
		298 K				
3		622	3275	0.029	0.46	
2		710	400	$<10^{-4}$		
1		670	3800	$<10^{-3}$	0.07	
0		639	3375	0.48	0.71	
				0.049 [b]		
$Ru(bpy)_n(bpz)_{3-n}^{2+}$						[154]
		298 K				
3		622	3275	0.029	0.46	
2		710	800	$<10^{-4}$		
1		654	2100	0.035	0.18	
				0.0043 [b]		
0		610	3275	0.45	0.74	
$Ru(bpm)_n(bpz)_{3-n}^{2+}$						[154]
		298 K				
3		639	3375	0.048 [b]	0.71	
2		655	3850	0.091 [b]	0.28	
1		633	3917	0.24 [b]	0.51	
0		610	3325	0.35 [b]	0.72	
$Ru(bpy)_n(pypm)_{3-n}^{2+}$						[147]
		298 K				
3		620	3960	0.0021	0.46	
2		649	550	0.0039		
1		636	483	0.0066		
0		620	3340	0.0078	0.81	
$Ru(bpy)_n(BL)_{3-n}^{2+}$						[144]
		298 K				
3		622	3275	0.0021		
2		770	789	$<10^{-4}$	0.98	
1		767	1417	7.6×10^{-4}	0.71	
0		762	1128	0.029	0.92	
$Ru(bpy)_n(biq)_{3-n}^{2+}$						[137]
	84 K					
3	583		4040		0.46	
2	~710		410			
0	~705		2690		0.98	
$Ru(bpy)_n(4\text{-}4'\text{-dpb})_{3-n}^{2+}$						[221]
	90 K	298 K				
3	575	617	3960		0.46	
2	600	628	4100		0.50	
1	616	631	4300		0.21	
0	606	638	4700		0.035	

[a] LC emission.
[b] [241].

difference in the mixed ligand complexes is larger than in the homoliganded members of the series. The variation of the activation parameters in the $Ru(bpy)_n(bpz)_{3-n}^{2+}$ series is similar. In none of the other series included in Table 3 is the distinction between homo- and heteroliganded complexes so sharply drawn.

Within each of the $Ru(bpy)_n(bpm)_{3-n}^{2+}$, $Ru(bpy)_n(bpz)_{3-n}^{2+}$, and $Ru(bpy)_n(BL)_{3-n}^{2+}$ series a small E_1 is roughly correlated with a relatively small emission energy, but this correlation is absent n the $Ru(bpy)_n(pypm)_{3-n}^{2+}$ sequence.

The interpretation of the dependence on n is complicated by the fact that the ^{3}MC level is influenced by the totality of the coordinated ligands [152] while the ^{3}MLCT level reflects the difference in the orbital energies of Ru(II) and the lowest unoccupied orbital of the ligand involved in the emission.

When the B ligands do not have low-lying π* orbitals that lead to low energy localized ^{3}MLCT transitions, they behave as spectator ligands that have little effect on k_{relax} [39].

4.2.1.4. Photoreaction and the population of ^{3}MC. $\eta_{bc} = A_1\exp(-E_1/k_BT)/[k_0 + A_1\exp(-E_1/k_BT)]$ represents the fraction of ^{3}MLCT that decays via ^{3}MC (Table 3) [153,154]. It includes recycling between the two levels and is not necessarily equal to $k_{bc}/(k_{bc}+k_{cb})$. There is no connection between Φ_{rx}, η_{bc}, and E_1 whether ^{3}MC or $^3MLCT_{4th}$ is the principal depopulation pathway. This might seem to be inconsistent with the generally accepted notion that photoreaction originates mainly in ^{3}MC. However, competition between reactive and nonradiative processes in ^{3}MC makes a direct correlation between η_{bc} and Φ_{rx} unlikely.

Appending an aromatic group with a triplet level slightly below ^{3}MLCT leads to a lengthening of the lifetime by reversible energy transfer [155,156]. When the aromatic triplet energy is too low for efficient energy transfer, the situation is more complex. For example, the emission spectrum of $Ru(bpy)_3^{2+}$ with a pyrene substituent separated by a methylene group changes slightly with delay time at 77 K in an alcohol glass [156]. The emission decay of this complex is nonexponential and this behavior has been ascribed to multiple emission. However, the time-resolved emission is invariant to delay time at r.t.

The luminescence of $Ru(bpy)_2(pztr)^+$ appears to meet the criteria for multiple emission [70]. Two bands with varying relative intensities and lifetimes persist in a fluid solution. The short lifetime is associated with the 590 nm band localized in the pyrazine part of $pztr^{-1}$. This decay is very temperature dependent in the interval 120–200 K ($A = 2\times10^{10}$ s^{-1}, $E = 850$ cm^{-1}). The long lifetime emission, presumed to be localized in bpy, changes little with temperature ($A = 6.5\times10^{6}$ s^{-1}, $E =$ 80 cm^{-1}). The 710 nm band disappears when the temperature in EM is lowered from 135 to 90 K, an unusual result, and the decay becomes exponential. Multiple emission would be expected to persist at low temperatures.

Non thermalization between an emissive and a nonemissive level has been suggested for $Ru(bpy)_2(dmpbq)^{2+}$ [9].

The picture which emerges from the Ru(II) results, contains the following elements: (1) thermalization in the lowest three ^{3}MLCT levels leads to an increase in k_{relax} with temperature. An activation energy < 100 cm^{-1} is expected; (2) at higher temperatures, two processes compete—population of $^3MLCT_{4th}$ and ^{3}MC levels. The former process is associated with $E_1 < 1000$ cm^{-1} and $A_1 < 10^9$ s^{-1}, while in the latter process $E_1 > 2800$ cm^{-1} and $A_1 > 10^{11}$ s^{-1}. Activation parameters between these limits are due to single-exponential fits when both processes are competitive; (3) the relative contributions of the two thermal decay processes depend upon the separation between the lowest ^{3}MLCT and the ^{3}MC levels; (4) in mixed ligand complexes energy transfer to the ligand with the lowest energy leads to localized emission from this ligand; (5) each ^{3}MLCT level is lowered by solvent motion but the same ordering still prevails.

4.2.2. Os(II) complexes

The excited state order in polypyridine complexes of Os(II) is the same as the Ru(II) analogs, but the energy separations are distinctly different. Ligand field strengths are ~30% higher in Os(II) leading to an increase in the ^{3}MC energy [3]. At the same time, the energy of the low-lying ^{3}MLCT manifold is reduced. Consequently, the emission is redshifted in an Os(II) complex compared with the Ru(II) twin and the ^{3}MLCT–^{3}MC gaps are much larger.

The temperature dependence of k_{relax} at low temperatures has been fitted to an equilibrium model [158] and only small E_1 (< 50 cm^{-1}) are again observed below 77 K.

There are few thermal activation parameters available for Os(II) complexes above 77 K (Table 4). Some of the fits were made with an equilibrium model while others were steady state. None of the activation energies exceeds 1000 cm^{-1}, indicating that the principal thermal decay pathway is via the $^3MLCT_{4th}$ level [138]. This conclusion is consistent with the large ^{3}MLCT–^{3}MC separations.

Rigidochromic effects obtain in this group of ^{3}MLCT emitters [159] and the enhanced k_{relax} induced by solvent motion fits the energy-gap law [160]. The small population of ^{3}MC at 298 K explains the relatively poor photoreactivity of most Os(II) complexes [159,161].

Table 4

Complex	Solvent	T Range	k_0 (s^{-1})	A (s^{-1})	E (cm^{-1})	Reference
$Os(bpy)_3^{2+}$	EM	210–298	3.70×10^6	7.2×10^7	312	[138]
$Os(bpy)_3^{2+}$	PB	90–298	0.62×10^6	6.4×10^7	330	[159]
$Os(bpy)_3^{2+}$	CA	77–298	4.2×10^6	1.9×10^8	607	[138]
$Os(bpy)_2(CH_3CN)_2^{2+}$	EM	77–298		2.05×10^7	221	[230]
$Os(bpy)_2(dppϕ)^{2+}$	EM	77–298		7.5×10^6	174	[230]
$Os(bpy)_2(diar)_2^{2+}$	EM	77–298		1.55×10^6	181	[230]
$Os(bpy)_2(CO)H^+$	EM	145–298	7.04×10^6	1.81×10^9	890	[225]
$Os(bpy)_2(CO)D^+$	EM	145–298	4.49×10^6	5.08×10^8	750	[225]
$Os(bpy)_2(CO)Cl^+$	EM	145–298	7.34×10^6	2.73×10^8	690	[225]
$Os(bpy)_2(dppe)^{2+}$	EM	140–298	0.55×10^6	0.8×10^7	291	[138]
$Os(bpy)_2(PPh_2me)_2^{2+}$	EM	150–298	0.8×10^6	2.5×10^7	492	[138]
$Os(phen)_2(das)^{2+}$	EM	160–298	1.6×10^6	1.4×10^7	600	[138]
$Os(bpy)_2(bpt)^+$	PB	90–298	3.9×10^6	7.8×10^7	440	[159]

Pairing with the counter ion affects the emission energy and k_{relax} at ambient temperatures in solvents with low dielectric constants [242].

$Os(biq)_2Cl_2$ is non-luminescent in a low temperature glass [162]. This was attributed to a low-lying ^{3}MC level due to a small ligand field strength.

4.2.3. Rh(III) complexes

Emission from Rh(III) complexes without azaaromatic ligands is ^{3}MC. The low temperature emission from $Rh(NH_3)_5X^{z+}$ ($X = NH_3$, NCS^-, and halides) is strong and the broad spectra are characteristic of the $^3T_1 \Rightarrow {}^1A_1$ transition [235,236], as are the emissions from other Rh(III) complexes without azaaromatic ligands [163].

Even when azaaromatics are coordinated, the large ionization energy of Rh(III) precludes population of ^{3}MLCT levels at ambient temperatures. The emission is often ^{3}MC, but structured ^{3}LC emission is observed in $Rh(bpy)_3^{3+}$, $Rh(phen)_3^{3=}$, and other complexes at low temperatures [47,164] (Table 5). The relative order of the ^{3}MC and ^{3}LC levels is sensitive to the ligand field strength of the non-azaaromatic ligands and the crossover between the emission from ^{3}LC to ^{3}MC has been observed when one NH_3 in $Rh(phen)_2(NH_3)_2^{3+}$ is replaced by Cl^- [165]. Both ^{3}MC and ^{3}LC emission is observed in $Rh(phen)_3^{3+}$ solutions at r.t. [239].

Rigidochromic redshifts are expected for ^{3}MLCT emitters, but comparison of an emission spectrum at two temperatures, in a glass and a fluid, is not sufficient to establish rigidochromism. Rigidochromic effects must first be distinguished from purely thermal variations. The change in an emission spectrum with temperature in a crystalline solid exemplifies a thermal effect. There is a redshift of the *cis*-$[Rh(en)_2Cl_2](NO_3)$ emission spectrum in the solid as the temperature is increased from 77 to 298 K [42]. This is a $^3MC \Rightarrow {}^1A_1$ transition and the spectral change was attributed to population of a second ^{3}MC level with a larger displacement of the potential minimum. A thermal broadening and *blueshift* is observed in *trans*-$[Rh(en)_2Cl_2](PF_6)$.

The $Rh(NH_3)_6^{3+}$ emission in glycerol is thermally broadened on the red-edge before the glycerol motion is appreciable and is not a rigidochromic effect [35]. The low temperature emission of this complex is broader in a $[Rh(NH_3)_6]Cl_3$ crystal than in the glass, but there is no thermal broadening. Other examples of thermally induced redshifts in a ^{3}MC emitter are *trans*-$Rh([15]aneN_4)(CN)_2^+$ in both a KBr matrix and an alcohol–water glass [166], $Rh(bpy)_2Br_2^+$ in glycerol [35], $[Rh(bpy)_2Cl_2](PF_6)$ [43], and $Rh(dpp)_2Cl_2^+$ [48]. The identification of an accessible second MC level is pertinent to the assessment of the thermal relaxation pathway [220].

Cyclometallation raises the ^{3}MC levels and the emission in $Rh(ppy)_2(bpy)^+$ and other complexes with ppy and thpy ligands is ^{3}LC [78,157,168].

Separation of $k(T)$ into $k_{nr}(T)$ and k_{rx} can be made when τ and Φ_{rx} are measured under the same conditions. Both measurements were made at r.t. for $Rh(NH_3)_5Cl^{2+}$, $Rh(en)_2XY$, and $Rh(NH_3)_4XY$ complexes [169–178]. In these reports Φ_{rx} was taken as the totality of the photoreaction, irrespective of the product. If k_0 is relatively small $k_{relax} = k(T)$, $k_{rx} = \Phi_{rx}/\tau$ and $k_{nr}(T) = k_{relax} - k_{rx}$. In this approach $k_{nr}(T)$ represents all thermal decay that does not lead to detectable products and may include transitions to higher ^{3}MC levels. Sometimes k_{rx} is the major contributor to k_{relax} at r.t. but not always [171,173,174]. Since the primary product is assumed to be a five-coordinate species there is always the question about the relationship between Φ_{rx} and the primary quantum yield, ϕ_{rx}. No consistent isomer effect has been established for either the absolute magnitudes or the relative values of the two rate constants.

In one case, measurements carried out over a limited temperature range yielded the thermal activation

parameters for $k_{nr}(T)$ in *trans*-$Rh(en)_2Br_2^+$ [172]. $k_{nr}(T)$ and $k_{rx}(T)$ were adequately represented by one-term functions, but the different activation energies, 920 and 2225 cm^{-1}, lead to non-Arrhenius behavior for $k(T)$. The small temperature interval and few data points make the fits uncertain.

The inadequacy of a single term fit for the *trans*-$Rh(en)_2Br_2^+$ $k(T)$ suggests that the Table 5 parameters should be viewed with caution. Two terms were required for a good fit of the $Rh(thpy)_2(bpy)^+$ and $Rh(ppy)_2(bpy)^+$ data [168]. For the former complex $E_2 = 900$ cm^{-1} and $A_2 = 9 \times 10^5$ s^{-1}.

Comparison of the thermal effect on the emission decay of several dicyano derivatives of Rh(III) complexes with macrocyclic amine ligands has been made [166]. It was concluded that the major effect was due to a strong coupling mechanism for $k_{nr}(T)$. It was also inferred from molecular mechanics calculations that *trans*-$Rh(cyclam)(CN)_2^+$ was more resistant to excited state distortion than either the *cis* analog or *trans*-$Rh([15]ane\ N_4)(CN)_2^+$, a factor that led to a higher activation energy.

Although there are few data on the effect of environmental rigidity, the incorporation of $Rh(NH_3)_6^{3+}$, $Rh(NH_3)_5Cl^{2+}$, and $Rh(cyclam)Cl_2^+$ into a crystal reduces both E and A when compared with a fluid medium. Since the crystals are not dilute, it is possible that the activation parameters do not represent purely intramolecular processes.

The behavior of $Rh(tpy)_2^{3+}$, $Rh(tpy)(bpy)(py)^{3+}$, and $Rh(tpy)(bpy)Cl^{2+}$, ^3MC emitters, is noteworthy [125]. The E values are very small in these species. In fact no $Rh(tpy)_2^{3+}$ emission was detectable at ambient temperatures. The change of emission from ^3LC in $Rh(bpy)_3^{3+}$ to ^3MC in $Rh(tpy)_2^{3+}$ is consistent with a distortion induced ligand field strength reduction when tpy is coordinated.fl

Table 5

Complex	Solvent	T Range (K)	k_0 (s^{-1})	A (s^{-1})	E (cm^{-1})		Reference
$Rh(NH_3)_6^{3+}$	EGW	77–193	5.0×10^4	2×10^{10}	1500	^3MC	[35]
$[Rh(NH_3)_6](ClO_4)_3$		85–295	2.6×10^4	0.08×10^7	420	^3MC	[207]
$[Rh(ND_3)_6](ClO_4)_3$		85–295	1.0×10^3	0.03×10^7	518	^3MC	[207]
t-$Rh(cyclam)(CN)_2^+$	MeOH–H_2O	77–298	6.4×10^5	6.2×10^{10}	2240	^3MC	[166]
c-$Rh(cyclam)(CN)_2^+$	MeOH–H_2O	77–298	5.9×10^4	6.3×10^9	1120	^3MC	[166]
t-$Rh(cyclam)(CN)_2^+$	MeOD–D_2O	77–298	1.6×10^3	1.3×10^9	2300	^3MC	[166]
t-$Rh(cyclam)(CN)_2^+$	EGW	77–298	7.1×10^3	9.6×10^{10}	2830	^3MC	[166]
t-$[Rh(cyclam)(CN)_2](ClO)_4$	KBr	77–300	7.5×10^3	7.8×10^9	1750	^3MC	[166]
t-$Rh([15]aneN_4)(CN)_2)(ClO)_4$	KBr	77–300	2×10^4	4.6×10^8	1670	^3MC	[166]
t-$Rh([15]aneN_4)(CN)_2^+$	MeOH–H_2O	77–298	2.2×10^4	7.2×10^8	1460	^3MC	[166]
$Rh(NH_3)_5Cl^{2+}$	H_2O	274–300			1890	^3MC	[227]
$[Rh(NH_3)_5Cl](ClO_4)_2$		85–295	9.1×10^4	1.3×10^7	664	^3MC	[207]
$[Rh(ND_3)_5Cl](ClO_4)_2$		85–295	2.1×10^3	0.8×10^7	769	^3MC	[207]
$[Rh(NH_3)_5Br](ClO_4)_2$		85–295	6.9×10^4	0.5×10^7	524	^3MC	[207]
$[Rh(ND_3)_5Br](ClO_4)_2$		85–295	2.7×10^3	0.08×10^7	594	^3MC	[207]
$Rh(thpy)_2(bpy)^+$	PB	77–310	1.9×10^3	2×10^{13}	3500	^3LC	[168]
$Rh(ppy)_2(bpy)^+$	PB	77–310	6.1×10^3	2×10^{14}	2600	^3LC	[168]
c-$[Rh(bpy)_2Cl_2](PF_6)$		350–536	2.2×10^4	7×10^{11}	4400	^3MC	[167]
c-$[Rh(bpy)_2Cl_2](PF_6)$		150–300	1.0×10^4	1.5×10^6	853	^3MC	[167]
c-$[Rh(phen)_2Cl_2](PF_6)$		350–536		1.5×10^{11}	3400	^3MC	[167]
c-$[Rh(phen)_2Cl_2](PF_6)$		150–300	1.4×10^4	1.6×10^6	860	^3MC	[167]
c-$[Rh(en)_2Cl_2](NO_3)$		300–497		6×10^{10}	2750	^3MC	[42]
c-$[Rh(en)_2Cl_2](NO_3)$		150–300	5.6×10^4	2×10^7	710	^3MC	[42]
t-$[Rh(en)_2Cl_2](PF_6)$		300–497		2×10^{11}	3100	^3MC	[42]
t-$Rh(en)_2Br_2^+$	H_2O	280–309		3.8×10^{10}	920	^3MC	[172] [b]
$Rh(bpy)_3^{3+}$	EM	77–310	4.5×10^2	6×10^{12}	2200	^3LC	168
$Rh(phen)_3^{3+}$	CH_3CN			10^{11}	2107	^3LC	168
$Rh(phen)_3^{3+}$	Glycerol	185–206			2800	^3LC	[14] [a]
$Rh(4\text{-mephen})_3^{3+}$	Glycerol	185–206			2500	^3LC	[14] [a]
$Rh(4,7\text{-me}_2\text{phen})_3^{3+}$	Glycerol	185–206			2900	^3LC	[14] [a]
$Rh(4,7\text{-me}_2\text{phen})_3^{3+}$	CH_3CN			10^{11}	2410	^3LC	[168]
$Rh(3,4,7,8\text{-me}_4\text{phen})_3^{3+}$	Glycerol	185–206			3800	^3LC	[14] [a]
$Rh(bpy)_2Br_2^+$	PG	77–236	4.3×10^4	5×10^{11}	1740	^3MC	[35]
$Rh(tpy)(bpy)(py)^{3+}$	H_2O	275–308			490	^3MC	[125]
$Rh(tpy)(bpy)Cl^{2+}$	H_2O	275–308			630	^3MC	[125]

[a] From rate of reaction.
[b] From $k_{nr}(T)$.

The Table 5 results suggest that two thermally activated processes contribute to the relaxation of some ^{3}MC states. One process, characterized by $E < 1000$ cm^{-1} and $A \approx 10^7$ s^{-1} dominates below ambient temperatures while at higher temperatures a second process with larger E and A is revealed. There are some complexes that do not appear to conform to this model but the possibility of fitting errors must be kept in mind. E and A for ^{3}LC emitters are much higher and suggest a relaxation pathway via ^{3}MC.

The decay behavior of the ^{3}LC emitters $Rh(bpy)_n(phen)_{3-n}^{3+}$ has been described in Section 2.9. The decay in a glass at 77 K that was exponential in the homoliganded pair became nonexponential in the heteroliganded species [67]. Examination of the Ir(III) analogues (v. infra) pointed to environmental heterogeneity rather than multiple emission as the source of the nonexponentiality [68].

4.2.4. Ir(III) complexes

In an early work, all three types of emission were assigned to the luminescence of Ir(III) complexes in glasses at 77 K [177]. The emission in both $Ir(phen)_3^{3+}$ and $Ir(tpy)_2^{3+}$ at 77 K and r.t. was assigned as ^{3}LC [150]. The levels of different orbital parentage are often proximate and the ordering very sensitive to small changes in the ligands [65]. In particular, the structured spectrum of $Ir(5,6\text{-}me_2\text{-}phen)_2Cl_2^+$ was assigned as ^{3}LC and the similarly structured emission from $Ir(phen)_2Cl_2^+$ was described as ^{3}MLCT. The major reason for the distinction was the large difference in the radiative lifetimes. The assignment of the $Ir(5,6\text{-}me_2\text{-}phen)_2Cl_2^+$ emission ^{3}LC has been confirmed, but mixing with ^{3}MLCT is significant [178].

The close similarity between the structured emissions of $Ir(bpy)_3^{3+}$, assigned as ^{3}LC, and those of $Ir(bpy)_2(acac)^{3+}$ and $Ir(bpy)_2(MeOH)^{3+}$, classified as ^{3}MLCT, again indicates that spectral shape is not always reliable in making the assignments [30]. The 77 K spectra of $Ir(bpy)_3^{3+}$ and $Ir(bpy)_2(MeOH)_2^{3+}$ in a glass are identical. However, the five-line Zeeman pattern of $Ir(bpy)_3^{3+}$ under resonant narrow band excitation supports a ^{3}LC assignment and the absence of such a Zeeman pattern for $Ir(bpy)_2(MeOH)_2^{3+}$ points to ^{3}MLCT emission [30]. The low temperature lifetimes of the two complexes are very different. The assignment of the structured emission of $Ir(bpy)_2(acac)$ as ^{3}MLCT was based on the same approach [243].

In one analysis of the emission from Rh(III) and Ir(III) complexes with cyclometallated ligands, the structured emission was always interpreted as ^{3}LC and the broad emission as ^{3}MLCT [78]. The increased ^{3}MC energy induced by ligand cyclometallation eliminates MC emission [179], but the energies of ^{3}MLCT and ^{3}LC may be so close in cyclometallated Ir(III) complexes that the emission can originate in either or both depending on the ligands and environment [78]. In $Ir(thpy)_2(bpy)^+$, this proximity leads to level inversion between rigid and fluid media; the emission changes from ^{3}LC at low temperatures in PMM to ^{3}MLCT in a fluid. Level inversion is also evident in $Ir(ppy)_2(NN)^+$ (NN = bpy, phen) and $Ir(bzq)_2(NN)^+$ [182]. The differential shift in ^{3}MLCT and ^{3}LC with fluidity explains the change in the $Ir(ppy)(bpy)_2^{2+}$ emission from structured to unstructured without any major redshift [180].

The emission spectra have been recorded for $Ir(tpy)_2^{3+}$ and a derivative in BN over a temperature range that includes the transition from the slow to fast solvent motion [49]. The emission of $Ir(tpy)_2^{3+}$ was assigned as ^{3}LC and exhibits no rigidochromic effect. The emission spectrum in $Ir(ttpy)_2^{3+}$ has much less structure and is redshifted by solvent motion, suggesting ^{3}MLCT as the emitting level. Substitution of pyridine on tpy appears to retain the ^{3}LC character of the emission [244], but with an aryl substituent (ttpy) the structure is reduced [49]. The emitting level in $Ir(ttpy)_2^{3+}$ may involve a contribution from ^{3}MLCT. In both cases there is an inflection in $k(T)$ similar to those observed in Ru(II) complexes but the break occurs after the solvent is very fluid. The origin for this break in a ^{3}LC emitter is not clear.

Only a few activation parameters have been published. $k(T)$ has been fitted for the ^{3}LC emission of the tpy and ttpy complexes in BN in the range 95–298 K [49]. The parameters are: $Ir(tpy)_2^{3+}$, $E = 1790$ cm^{-1} and $A = 7.6 \times 10^9$ s^{-1}; $Ir(ttpy)_2^{3+}$, $E = 1040$ cm^{-1} and $A = 2.2 \times 10^7$ s^{-1}.

The effect of environment on the energy levels is also relevant to the interpretation of multiple emission, which has been suggested to explain the nonexponential decay of several heteroliganded cyclometallated Ir(III) complexes, $Ir(bzq)_2(NN)^+$ and $Ir(ppy)_2(NN)^+$ (NN = bpy, phen) in rigid glasses [182]. In the multiple emission interpretation there is incomplete thermalization between two ^{3}MLCT levels. An alternative explanation for the nonexponential decay involving environmental heterogeneity has been advanced [78]. In this model the narrow ^{3}LC energy distribution is overlapped by a broad ^{3}MLCT distribution and emission from both levels is superimposed. In a crystalline environment and in fluid solutions, the decays are exponential at all excitation wave lengths, evidence against multiple emission.

The bpy and phen ^{3}LC levels in $[Ir(bpy)_n(phen)_{3-n}]^{3+}$ ($n = 1, 2$) complexes differ little in energy. In particular, the origin bands are nearly coincident [30,68]. Bpy is preferentially excited upon irradiation in the origin bands, yet both phen and bpy emit in the same way as when the UV bands are irradiated. If multiple emission occurred, excitation in bpy would yield only bpy emission. The inhomogeneous widths of the bpy and phen energies are larger than the energy

difference between the centroids of the distributions. Consequently, in some complexes phen is the lower while in others bpy is lower. The nonexponentiality in the emission of the heteroliganded complexes is then due to environmental heterogeneity.

$Ir(bpy)_2Cl_2^+$ is another case of putative multiple emission from ^{3}MLCT and ^{3}MC levels [73]. However, nonexponentiality is found only in rigid media and this interpretation has been questioned [69].

4.2.5. Re(I) complexes

These complexes are designated as organometallics since stability requires coordination of ligands like CO in addition to those bonded in the usual Werner fashion. Nonetheless, the excited states can be described in terms of orbital parentage as in other d^6 complexes. The main effect of CO is to raise the ^{3}MC levels and when azaaromatics are coordinated the d^6 energy level model with ^{3}MLCT or ^{3}LC emission has proven to be adequate. A rigidochromic effect is again diagnostic of ^{3}MLCT emission [183].

^{3}MLCT emission predominates in fluids, but this does not require that ^{3}MLCT be the lowest level. The larger radiative rate in ^{3}MLCT compared with ^{3}LC means that thermal population of ^{3}MLCT can lead to dominant emission from that level even though higher in energy [184]. Site heterogeneity often produces time-dependent emission spectra in rigid media.

k_{relax} of $Re(NN)(CO)_3Cl$ was fitted to Eq. (16) between 4 and 77 K with the characteristic ^{3}MLCT sublevel splittings [185].

The emission properties of Re(I) complexes have been reviewed [65,186,187]. Re(I) tricarbonyl complexes have received the most attention. Studies of the effect of temperature on emission properties have usually been carried out at two temperatures, 77 K and ambient. Criteria for assigning the emission have been advanced [188]. In some complexes, the 77 K emission is ^{3}LC but the proximity of ^{3}MLCT and ^{3}LC coupled with the rigidochromism of ^{3}MLCT leads to level inversion during the rigid-fluid transition [189,190]. In one complex, $Re(DEAS\text{-}bpy)(CO)_3Cl$, the 77 K structured spectrum becomes broad and structureless at 293 K without much change in energy [188]. The emission was assigned as ^{3}LC at both temperatures, but this is questionable.

In $Re(NN)(CO)_3Cl$ complexes (NN = substituted bpy) either ^{3}MLCT or ^{3}LC emission occurred in a rigid glass [188]. In one case, emission from both ^{3}MLCT and ^{3}LC was resolved in a rigid medium. This could arise from environmental heterogeneity wherein the ^{3}LC and the broadened ^{3}MLCT levels overlap.

The emission spectra of a group of $Re(NN)(CO)_3py^+$ complexes, where NN was a methyl or phenyl substituted phenanthroline, have been recorded at 77 K and r.t. [191,192]. The order and separation of ^{3}LC and ^{3}MLCT was sensitive to substituent changes on the phen moiety. ^{3}MLCT emission was always dominant at r.t. and the decays were exponential. In a rigid environment at 77 K some complexes were still ^{3}MLCT emitters while others exhibited the characteristic ^{3}LC spectrum. The spectra varied with the excitation wave length and delay time; nonexponential decay kinetics obtained. Again, environmental heterogeneity played an important role in the excited state ordering and there was no multiple emission. In the time resolved spectra of some complexes, the broad ^{3}MLCT emission at short delay times was replaced by the structured ^{3}LC emission at longer delay.

The dependence of the decays on temperature was determined for the same group of complexes in fluid EM in the 150–315 K range [193]. With one exception (NN = 3,4,7,8-me_4phen), the decay could be fitted by a one-term equilibrium model with $E_1 = 120$–$900\ cm^{-1}$ and $A_1 \approx 10^6\ s^{-1}$. The small A_1 is consistent with equilibration. The upper level was not identified but it might be $(^3MLCT)_{4th}$. When NN = 3,4,7,8-me_4phen, a three-level model was required with $E_1 = 1430\ cm^{-1}$ and $E_2 = 130\ cm^{-1}$. E_2 was associated with ^{3}LC population.

Although ^{3}MLCT is usually the lowest excited level in fluid media, extensive delocalization onto an azaaromatic ligand can depress ^{3}LC below ^{3}MLCT [184]. The $Re(dppz)(CO)_3Cl$ emission is ^{3}MLCT even though ^{3}LC is lower in energy. This was ascribed to thermal population of ^{3}MLCT. ^{3}LC emission is observed in $[Re(dppz)(CO)_3(PPh_3)]^+$. ^{3}LC emission is obtained when other ligands with extensively delocalized π systems are coordinated [193,194].

The emission of $Re(NN)(CO)_4(PF_6)$ in PMM and in crystals (pure and dilute) has been assigned as ^{3}LC with some ^{1}MLCT mixing [196]. There was very little thermal decrease in the lifetime in the 20–298 K range ($\tau = 28.5$–33 μs) in the bpy complex. However, when NN = phen the lifetime was much longer (295 μs) at 20 K, due to decreased mixing with ^{3}MLCT. The thermal quenching of the phen complex emission indicates the accessibility of another level whose identity could not be established.

The emission of complexes with cyclometallated phen (bhq) exhibits some ^{3}LC structure at both low and r.t. with ms lifetimes at 77 K [237]. Similar behavior prevails in $Re(CO)_4(thpy)$ [195].

The assignment of the $ReL(CO)_4X$ (L = piperidine, PPh_3; X = Cl, I) emission as ^{3}MC is expected in the absence of an azaaromatic ligand [197]. This assignment was based on the correlation of the emission and absorption energies. The broad emission spectral positions do not exhibit the solvent sensitivity characteristic of ^{3}MLCT emission.

In addition to locating the several excited states, the extensive literature has been focused on identifying

multiple emissions. The overwhelming majority of purported multiple emissions in Re(I) complexes have been in rigid media at low temperatures, but a few cases have involved fluid solvents. Tricarbonyls with bisquinoline or pyridine derivatives as ligands exhibit nonexponential decays in fluid media and are apparently cases of multiple emission involving inhibition of intramolecular transitions from ^{3}LC to ^{3}MLCT [71]. There are contributions from both levels in the 298 K emission spectra.

k_{nr} in Re(I) complexes exhibits a dependence that follows the energy gap law [198].

4.2.6. Cr(0), Mo(0), and W(0) complexes

In an Ar matrix $Cr(CO)_6$ emits at 10 K only after population of $^3T_1$ by sensitization, indicating inefficient intersystem crossing [199]. Emission of this complex at 340–360 nm was assigned as fluorescence ($^1T_1 \Rightarrow {}^1A_1$) [200]. In fluid methanol (MeOH) fast dissociation occurs [240] and the emission is quenched, presumably by the photoreaction. Emission in Mo and W hexacarbonyls has also been observed in matrices at 12 K [200]. Thermal quenching is again efficient and no emission was detected in a glass at 77 K.

Substitution of one CO changes the picture dramatically. Emission in $W(CO)_5L$ ($L = Cl^-$, Br^-, I^-, NCO^-, CS) in a rigid solution is observed at 77 K with lifetimes in the 10–15 μs range [201]. Tungsten pentacarbonyl complexes with pyridine derivative ligands have low-lying ^{3}MLCT levels [202,203]. The ^{3}MC–^{3}MLCT order is sensitive to L. When L is py and some derivatives, ^{3}MC is the lowest with lifetimes near 1 μs; the order is reversed in other derivatives with 15–38 μs lifetimes. Φ_{rx} is much larger when ^{3}MC is the lower. Emission persists at 298 K for the ^{3}MLCT emitters with thermal activation parameters: $E_1 = 525$–1100 cm^{-1} and $A_1 \approx 10^8$ s^{-1} [203]. The emission intensity increases with temperature as the lifetime decreases, indicating involvement of more than one level. The higher level was assumed to also be ^{3}MLCT and to be responsible for most of the emission in fluid media. In this picture, the separation between the two ^{3}MLCT levels corresponds to E_1. In a few complexes, the involvement of a low-lying LMCT level has been inferred [204].

The excited state relaxation in $Mo(CO)_5L$ complexes (L = pyridine derivatives) parallels that in the corresponding W(0) species and was interpreted in terms of close lying ^{3}MC and ^{3}MLCT levels [205]. This proximity again leads to sensitivity of the excited state ordering to the substituent on the pyridine ligand. When ^{3}MLCT is lower, the emission persists at r.t. and Φ_{rx} is small.

Two bands are present in the r.t. and 80 K emission spectra of $W(CO)_4(NN)$ and $Mo(CO)_4(NN)$ with NN = phen, bpy and derivatives [77,238]. The lifetimes of the two emissions are different at 298 K, indicating incomplete thermalization, and both transitions were assigned as ^{3}MLCT. There is also a dependence of the 293 K emission spectra on the excitation wave length suggesting multiple emission. ^{3}MC emission was observed from $W(CO)_4(X)_2$ (X = py, en piperidine) at 77 K [206]. When X was bpy, phen, or substituted phen ^{3}MLCT was lower.

5. Summary and conclusions

The reliability of the thermal activation parameters is critically dependent on the quality of the kinetic data and the adequacy of the fitting model. It is essential to examine decay data over a wide temperature range in order to separate the contributions of competing relaxation processes. Kinetic arguments are seldom decisive in establishing the pathways for depopulation of excited electronic states. Nonetheless, when combined with spectral data they can be very helpful. Spectroscopic data alone are unreliable because potential surface barriers to kinetic processes are not always revealed by absorption spectra.

In Cr(III) complexes, relaxation of the lowest excited state involves MC levels. At low temperatures, nonradiative processes originating in ^{2}E dominate the relaxation when ^{2}E is lowest. Solvent motion facilitates excited state relaxation by changing state energies and potential surface anharmonicities. Back-intersystem crossing from ^{2}E to $^4T_2$ is energetically allowed and is the main source of $k(T)$ in nearly all of complexes in this class, but there are some exceptions. The absence of fluorescence does not rule out back-transfer. Environmental heterogeneity in a rigid matrix leads to nonexponentiality when $k(T)$ is significant. This is ascribed to a distribution of $^4T_2$–^{2}E gaps. A crystalline environment drastically reduces $k(T)$.

Only MC levels participate in the relaxation of d^6 complexes without ligands that have low-lying π* orbitals. Coordination of azaaromatics introduces ligand-localized and metal-to-ligand charge-transfer states. The ordering of these levels is sensitive to the ligands and to the environment. The classification in terms of orbital parentage is an approximation that is surprisingly useful in systemizing excited state relaxation behavior for a wide range of complexes involving coordination of many different ligands with varying metal ions.

Interligand energy transfer leads to localization in a single ligand prior to emission for ^{3}MLCT and ^{3}LC emitters. If several levels are proximate environmental heterogeneity in a rigid medium leads to nonexponentiality and emission from more than one level, but in

different complexes. This is not multiple emission from nonthermalized levels in the same complex.

When ^{3}MLCT is the emitting level, thermal changes below 77 K are the result of changing populations among the three lowest sublevels. Above 77 K, ^{3}MC and a fourth ^{3}MLCT level are competing relaxation pathways. When the lowest excited level is not ^{3}MLCT, emission is quenched within the manifold of ^{3}MC levels, while the thermal relaxation of ^{3}LC probably involves a ^{3}MC level.

Photochemistry is mainly the result of ^{3}MC population but the quantum yield is not a good indicator of the efficiency for the population of metal-centered levels since there is competition between nonradiative relaxation and photochemistry in ^{3}MC.

6. Solvents and abbreviations

BN	butyronitrile
C.A.	cellulose acetate
DMF	dimethylformamide
DMSO	dimethylsulfoxide
EM	ethanol–methanol 4:1 (v/v)
EGW	ethylene glycol–water 2:1 (v/v)
EtOH	ethanol
MeOH	methanol
PB	propionitrile–butyronitrile
PC	propylene carbonate
PEN	C_3H_7CN–C_2H_5CN 5:4 (v/v)
PG	propylene glycol
PMM	polymethylmethacralate

Ligand Structures

acac

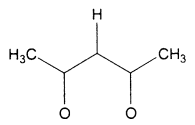

AEP

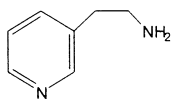

BCNE

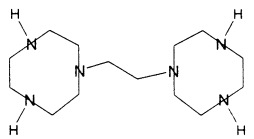

biq

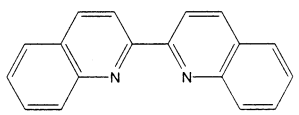

BL

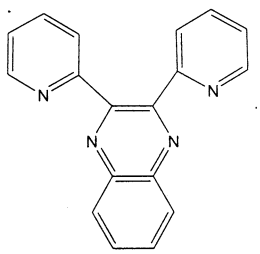

bpm

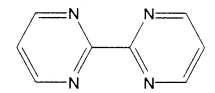

bpt

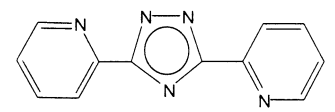

bpy

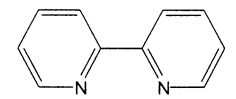

bpz

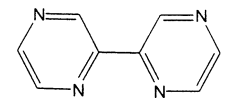

bzq

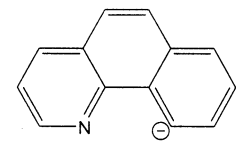

cyclam

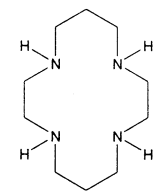

das

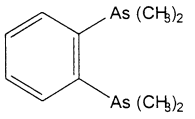

dcb

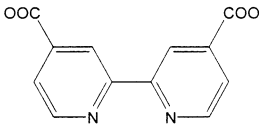

decb

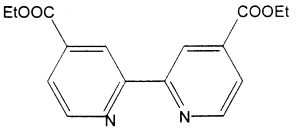

dhab

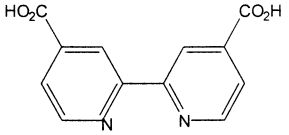

diaz

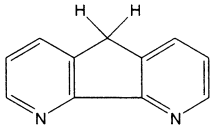

dmb

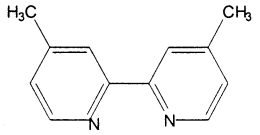

DMCH

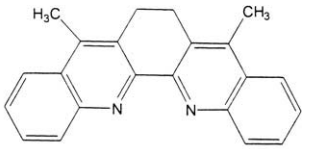

dmpbq

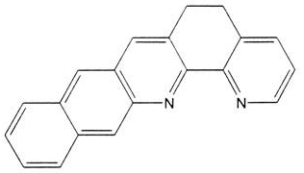

4, 4'-dpb

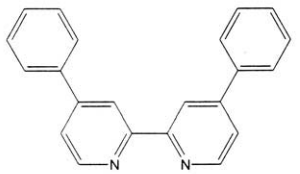

dpp

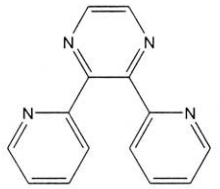

dppe

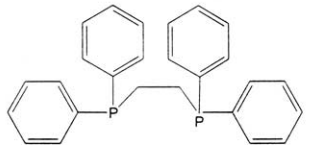

dppø

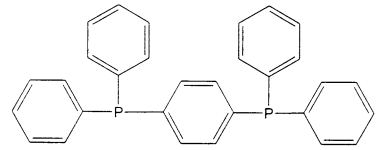

4, 4'-dpt

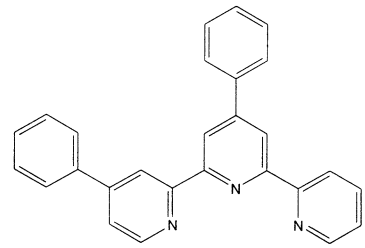

dppz

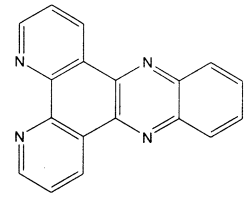

en

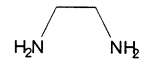

4-etpy

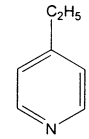

hat

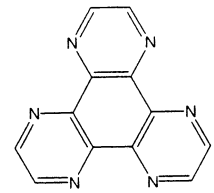

i-biq

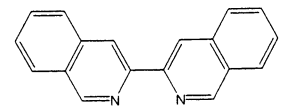

H3 Meptr

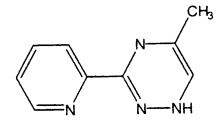

1 Meptr

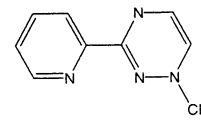

mmb

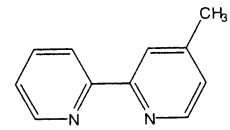

NMI

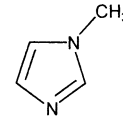

NPP 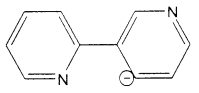

ox 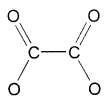

phen 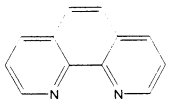

PPh_3 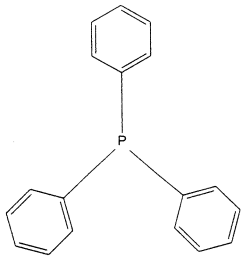

ppy 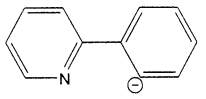

pq 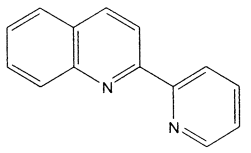

py 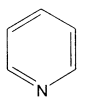

pyd 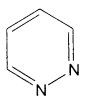

pypm 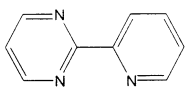

pypz 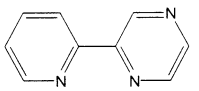

pztr 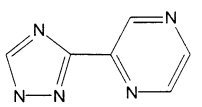

tap 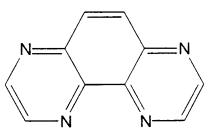

tetb 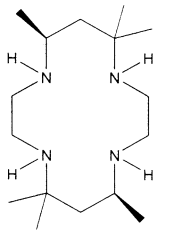

thpy 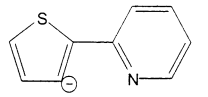

tpm 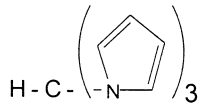

tpy 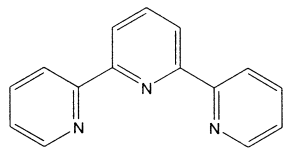

tsite 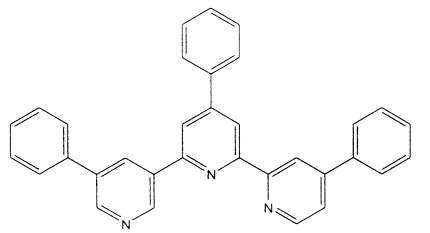

ttpy 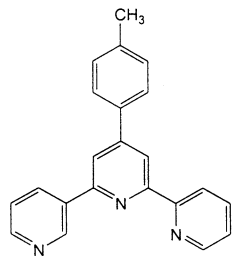

$[15]aneN_4$ 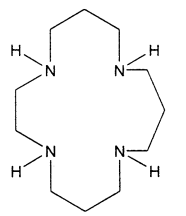

$[9]aneN_3$ 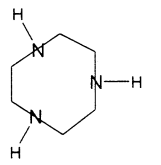

References

[1] T.J. Kemp, Prog. React. Kinet. 10 (1980) 301.
[2] J.F. Endicott, T. Ramasami, R. Tamilarasan, R.B. Lessard, C.K. Ryu, G.F. Brubaker, Coord. Chem. Rev. 77 (1987) 1.
[3] T.J. Meyer, Pure Appl. Chem. 58 (1986) 1193.
[4] A. Juris, V. Balzani, F. Barigelletti, E. Campagna, F. Belser, A. Von Zelewsky, Coord. Chem. Rev. 84 (1988) 85.
[5] A.D. Kirk, Chem. Rev. 99 (1999) 1607.
[6] S.W. Benson, The Foundations of Chemical Kinetics, McGraw-Hill, New York, 1960, p. 39.
[7] L.S. Forster, Chem. Rev. 90 (1990) 331.
[8] J.N. Demas, D.G. Taylor, Inorg. Chem. 18 (1979) 3177.
[9] E. Tafforel, S. Chiragil, W.Y. Kim, R.P. Thummel, R.H. Schmehl, Inorg. Chem. 35 (1996) 2177.
[10] J.R. Shaw, R.T. Webb, R.H. Schmehl, J. Am. Chem. Soc. 112 (1990) 1117.
[11] G.D. Hager, G.A. Crosby, J. Am. Chem. Soc. 97 (1975) 7031.
[12] R. Reisfeld, P. Brusilovsky, M. Eyal, C.K. Jørgensen, Chimia 43 (1989) 385.
[13] E. Becquerel, La Lumière, Firmin Didot, 1867.
[14] J.A. Brozik, G.A. Crosby, J. Phys. Chem. A 102 (1998) 45.
[15] J. Lakowicz, Principles of Fluorescence Spectroscopy, Plenum Press, New York, 1983.
[16] D.V. O'Connor, D. Phillips, Time-Correlated Single Photon Counting, Academic Press, London, 1984, p. 181.
[17] J.N. Demas, S.E. Demas, Interfacing and Scientific Computing on Personal Computers, Allyn & Bacon, Needham Hts, MA, 1996.
[18] W.H. Press, B.P. Flannery, S.A. Teukolsky, W.T. Vetterling, Numerical Recipes, Cambridge University Press, Cambridge, 1986 Chapter 14.
[19] J.N. Demas, G.A. Crosby, J. Phys. Chem. 75 (1971) 991.
[20] F. Barigelletti, A. Juris, V. Balzani, P. Belser, A. Von Zelewsky, J. Phys. Chem. 90 (1986) 5190.
[21] K.D. Mielenz, E.D. Cehelnik, R.L. McKenzie, J. Chem. Phys. 64 (1975) 370.
[22] J.R. Lakowicz, Z. Murtaza, W.E. Jones, K. Kim Jr, H. Szmacinski, J. Fluoresc. 6 (1996) 245.
[23] J.R. Lakowicz, E. Terpetschnig, Z. Murtaza, H. Szmacinski, J. Fluoresc. 7 (1997) 17.
[24] B.A. DeGraff, J.N. Demas, J. Phys. Chem. 98 (1994) 12478.
[25] H.-B. Kim, N. Kitamura, S. Tazuke, Chem. Phys. Lett. 143 (1988) 77.
[26] L.S. Forster, Inorg. Chim. Acta 277 (1998) 211.
[27] M. Adelt, M. Devenney, T.J. Meyer, D.W. Thompson, J.A. Treadway, Inorg. Chem. 37 (1998) 2616.
[28] W.E. Jones, P. Chen Jr., T.J. Meyer, J. Am. Chem. Soc. 114 (1992) 387.
[29] L.J. Andrews, A. Lempicki, B.C. McCollum, Chem. Phys. Lett. 74 (1980) 404.
[30] E. Krausz, H. Riesen, Coord. Chem. Rev. 159 (1997) 9.
[31] M. Sykora, J.R. Kincaid, Inorg. Chem. 34 (1995) 5852.
[32] R.B. Lessard, J.F. Endicott, M.W. Perkovic, L.A. Ochrymowyez, Inorg. Chem. 28 (1989) 2574.
[33] C.K. Ryu, J.F. Endicott, Inorg. Chem. 27 (1988) 2203.
[34] N.A.P. Kane-Maguire, K.C. Wallace, D.B. Miller, Inorg. Chem. 24 (1985) 597.
[35] L.S. Forster, unpublished.
[36] J.P. Claude, T.J. Meyer, J. Phys. Chem. 99 (1995) 51.
[37] J.V. Caspar, T.J. Meyer, J. Phys. Chem. 87 (1983) 952.
[38] E.M. Kober, J.V. Caspar, R.S. Lumpkin, T.J. Meyer, J. Phys. Chem. 90 (1986) 3722.
[39] J.V. Caspar, T.J. Meyer, Inorg. Chem. 22 (1983) 2444.
[40] S.H. Lin, J. Chem. Phys. 56 (1972) 2648.
[41] M.S. Wrighton, D.L. Morse, J. Am. Chem. Soc. 96 (1974) 998.
[42] A. Islam, N. Ikeda, K. Nozaki, T. Ohno, J. Chem. Phys. 109 (1998) 4900.
[43] A. Islam, N. Ikeda, K. Nozaki, T. Ohno, Chem. Phys. Lett. 263 (1996) 209.
[44] A.M. Ghaith, L.S. Forster, J.V. Rund, Phys. Chem. 92 (1988) 6197.
[45] P. Chen, T.J. Meyer, Chem. Rev. 98 (1998) 1439.
[46] A. Juris, F. Barigelletti, V. Balzani, P. Belser, A. Von Zelewsky, Inorg. Chem. 24 (1985) 202.
[47] D.H.W. Carstens, G.A. Crosby, J. Mol. Spectrosc. 34 (1970) 113.
[48] K. Kalyanasundaram, M. Grätzel, M.K. Nazeeruddin, J. Phys. Chem. 96 (1992) 5865.
[49] J.-P. Collin, I.M. Dixon, J.-P. Sauvage, J.A.G. Williams, F. Barigelletti, L. Flamigni, J. Am. Chem. Soc. 121 (1999) 5009.
[50] K. DeArmond, L.S. Forster, Spectrochim. Acta 19 (1963) 1395.
[51] F. Barigelletti, J. Chem. Soc. Faraday 2 (83) (1987) 1567.
[52] F. Bargelletti, P. Belser, A. Von Zelewsky, A. Juris, V. Balzani, J. Phys. Chem. 89 (1985) 3680.
[53] H. Riesen, L. Wallace, E. Krausz, J. Phys. Chem. 99 (1995) 16807.
[54] H. Yersin, W. Humbs, J. Strasser, Op. Curr. Chem. 191 (1977) 154.
[55] H. Yersin, W. Humbs, J. Strasser, Coord. Chem. Rev. 159 (1997) 325.
[56] H. Yersin, D. Braun, Coord. Chem. Rev. 111 (1991) 39.
[57] H. Riesen, E. Krausz, Comments Inorg. Chem. 18 (1995) 27.
[58] P. Huber, H. Yersin, J. Phys. Chem. 97 (1993) 12705.
[59] W. Humbs, H. Yersin, Inorg. Chem. 35 (1996) 2220.
[60] W. Humbs, J. Strasser, H. Yersin, J. Lumin. 677 (1997) 72.
[61] P.G. Bradley, N. Kress, B.A. Hornberger, R.F. Dallinger, W.H. Woodruff, J. Am. Chem. Soc. 103 (1981) 7441.
[62] J.R. Schoonover, C.A. Bignozzi, T.J. Meyer, Coord. Chem. Rev. 165 (1997) 239.
[63] J.R. Schoonover, K.M. Ornberg, J.A. Moss, S. Bernhard, V.J. Malvey, W.H. Woodruff, T.J. Meyer, Inorg. Chem. 37 (1998) 2585.
[64] J.L. Pogge, D.F. Kelley, Chem. Phys. Lett. 238 (1995) 16.
[65] K. Kalyanasundaram, Photochemistry of Polypyridine and Porphyrin Complexes, Academic Press, London, 1992.
[66] A. Juris, F. Bargelletti, V. Balzani, P. Belzer, A. Von Zelewsky, J. Chem. Soc. Faraday 2 (83) (1987) 295.
[67] G.A. Crosby, W.H. Elfring Jr., J. Phys. Chem. 80 (1976) 2206.
[68] E. Krausz, J. Higgins, H. Riesen, Inorg. Chem. 32 (1993) 4053.
[69] L. Wallace, G.A. Heath, E. Krausz, G. Moran, Inorg. Chem. 30 (1991) 347.
[70] T.E. Keyes, C.M. O'Connor, U. O'Dwyer, C.G. Coates, P. Callaghan, J.J. McGarvey, J.G. Vos, J. Phys. Chem. A 103 (1999) 8915.
[71] G. Ferraudi, M. Feliz, E. Wolson, I. Hsu, S.A. Moya, J. Guerrero, J. Phys. Chem. 99 (1995) 4929.
[72] L. Wallace, C. Woods, D.P. Rillema, Inorg. Chem. 34 (1995) 2875.
[73] R.J. Watts, S. Efrima, H. Metiu, J. Am. Chem. Soc. 101 (1979) 2742.
[74] B. Divisio, P.C. Ford, R.J. Watts, J. Am. Chem. Soc. 102 (1980) 7264.
[75] R.J. Watts, J. Am. Chem. Soc. 96 (1974) 6186.
[76] R.J. Watts, D. Missimer, J. Am. Chem. Soc. 100 (1978) 5350.
[77] K.A. Rawlins, A.J. Lees, Inorg. Chem. 28 (1989) 2154.
[78] M.G. Colombo, A. Hauser, H.U. Güdel, Top Curr. Chem. 171 (1994) 143.
[79] J.F. Endicott, M.W. Perkovic, M.J. Heeg, Adv. Chem. Ser. 253 (1997) 199.
[80] F. Castelli, L.S. Forster, Phys. Rev. B 11 (1975) 920.
[81] D.A. Friesen, S.H. Lee, R.E. Naslaem, S.P. Mezyk, W.L. Waltz, Inorg. Chem. 34 (1995) 4046.

[82] C.D. Flint, A.P. Matthews, J. Chem. Soc. Faraday 2 (69) (1973) 419.
[83] A.M. Ghaith, L.S. Forster, J.V. Rund, Inorg. Chem. 26 (1987) 2493.
[84] G.E. Rojas, D. Magde, Inorg. Chem. 26 (1987) 2334.
[85] G.B. Porter, H.L. Schläfer, Z. Phys. Chem. (Frankfurt) 37 (1963) 109.
[86] D.M. Klassen, H.L. Schläfer, Ber. Bunsenges Physik. Chem. 72 (1968) 663.
[87] L.S. Forster, J.V. Rund, F. Castelli, P. Adams, J. Phys. Chem. 86 (1982) 2395.
[88] F.D. Camassei, L.S. Forster, J. Chem. Phys. 50 (1969) 2603.
[89] S. Brönnemann, A. Zilian, H.U. Güdel, A. Ludi, Inorg. Chim. Acta 173 (1990) 159.
[90] A.R. Gutíerrez, A.W. Adamson, J. Phys. Chem. 82 (1978) 902.
[91] A.D. Kirk, Comments Inorg. Chem. 14 (1993) 89.
[92] L.S. Forster, Inorg. Chim. Acta 247 (1996) 1.
[93] L.S. Forster, J. Vandermark, J.V. Rund, Inorg. Chim. Acta 202 (1992) 141.
[94] L.S. Forster, D. Murrow, A.F. Fucaloro, Inorg. Chem. 29 (1990) 3706.
[95] M.W. Perkovic, M.J. Heeg, J.F. Endicott, Inorg. Chem. 30 (1991) 3140.
[96] J.F. Endicott, R. Tamilarasan, R.B. Lessard, Chem. Phys. Lett. 112 (1984) 381.
[97] M.W. Perkovic, J.F. Endicott, J. Phys. Chem. 94 (1990) 1217.
[98] A.D. Kirk, H.U. Güdel, Inorg. Chem. 31 (1992) 4564.
[99] R.B. Lessard, T. Buranda, M.W. Perkovic, C.L. Schwarz, Y. Rudong, J.F. Endicott, Inorg. Chem. 31 (1992) 3091.
[100] D.F. Friesen, S.H. Lee, J. Lilie, W.L. Waltz, L. Vincze, Inorg. Chem. 30 (1991) 1975.
[101] W.L. Waltz, Private Communication.
[102] K.N. Brown, R.J. Geue, G. Moran, S.F. Ralph, H. Riessen, A.M. Sargeson, J. Chem. Soc. Chem. Comm. 1998, 2291.
[103] P. Comba, I.I. Creaser, L.R. Gahan, J. MacB Harrowfield, G.A. Lawrence, L.L. Martin, A.W.H. Mau, A.M. Sargeson, W.H.F. Sasse, M.R. Snow, Inorg. Chem. 26 (1986) 384.
[104] P. Comba, A.W.H. Mau, A.M. Sargeson, J. Phys. Chem. 89 (1985) 394.
[105] H. Wasgestion, J. Phys. Chem. 76 (1972) 1947.
[106] R. Dannöhl-Fickler, H. Kelm, F. Wasgestion, J. Lumin. 10 (1975) 103.
[107] H.W. Bückels, F. Wasgestion, Ber. Bunsenges. Phys. Chem. 87 (1983) 154.
[108] K. Maruszewski, D. Andrzhwski, W. Strek, J. Lumin. 72–74 (1997) 226.
[109] H. Yersin, H. Otto, G. Gliemann, Theoret. Chim. Acta 33 (1974) 63.
[110] F. Castelli, L.S. Forster, J. Am. Chem. Soc. 97 (1975) 6306.
[111] A.F. Fucaloro, L.S. Forster, J.V. Rund, S.H. Lin, J. Phys. Chem. 87 (1983) 1796.
[112] S.S. Shah, A.W. Maverick, Inorg. Chem. 25 (1986) 1867.
[113] A.F. Fucaloro, L.S. Forster, S.G. Glover, A.D. Kirk, Inorg. Chem. 24 (1985) 4242.
[114] C.D. Flint, A.P. Mathews, Inorg. Chem. 14 (1975) 1008.
[115] C.D. Flint, A.P. Mathews, J. Chem. Soc. Faraday 2 (70) (1974) 1307.
[116] W.L. Waltz, J. Lilie, S.H. Lee, Inorg. Chem. 23 (1984) 1768.
[117] C.H. Langford, Accts. Chem. Res. 17 (1984) 96.
[118] G.A. Crosby, Accts. Chem. Res. 8 (1975) 231.
[119] A. Juris, S. Campagna, V. Balzani, G. Gremaud, A. von Zelewsky, Inorg. Chem. 27 (1988) 3652.
[120] H. Riesen, E. Krausz, L. Wallace, J. Phys. Chem. 96 (1992) 3621.
[121] M.G. Colombo, T.C. Brunold, T. Riedener, H.U. Güdel, Inorg. Chem. 33 (1994) 545.
[122] S. Campagna, A. Bartolotta, G. DiMarco, Chem. Phys. Lett. 206 (1993) 30.
[123] R.J. Watts, G.A. Crosby, J.L. Sansregret, Inorg. Chem. 11 (1972) 1414.
[124] G.A. Crosby, K.W. Hipps, W.H. Elfring Jr., J. Am. Chem. Soc. 96 (1974) 629.
[125] M.E. Frink, S.D. Sprouse, H.A. Goodwin, R.J. Watts, P.C. Ford, Inorg. Chem. 27 (1988) 1283.
[126] C.H. Langford, A.Y.S. Malkhasion, J. Am. Chem. Soc. 109 (1987) 2682.
[127] E.I. Solomon, A.B.P. Lever, Electronic Absorption Spectroscopy, vol. 2, Wiley, New York, 1999, p. 291.
[128] F. Barigelletti, L. De Cola, A. Juris, Gazz. Chim. Ital. 120 (1990) 545.
[129] P. Belser, A. von Zelewsky, A. Juris, F. Barigelletti, A. Tucci, V. Balzani, Chem. Phys. Lett. 89 (1982) 101.
[130] S. Kimachi, R. Satomi, H. Miki, K. Maeda, T. Azumi, M. Onishi, J. Phys. Chem. A101 (1997) 345.
[131] P. Belser, A. von Zelewsky, A. Juris, F. Barigelletti, V. Balzani, Gazz. Chim. Ital. 113 (1983) 731.
[132] H.-B. Kim, N. Katamura, S. Tazuke, J. Phys. Chem. 94 (1990) 7401.
[133] E. Krausz, J. Ferguson, Prog. Inorg. Chem. 37 (1989) 293.
[134] Y. Komoda, S. Yamauchi, N. Hirota, J. Phys. Chem. 92 (1988) 6511.
[135] M. Maestri, N. Armaroli, V. Balzani, E.C. Constable, A.M.W. Thompson, Inorg. Chem. 34 (1995) 2759.
[136] F. Barigelletti, A. Juris, V. Balzani, P. Belser, A. von Zelewsky, J. Phys. Chem. 91 (1987) 1095.
[137] F. Barigelletti, A. Juris, A. Balzani, P. Belser, A. von Zelewsky, Inorg. Chem. 22 (1983) 3335.
[138] R.S. Lumpkin, E.M. Kober, L.A. Worl, Z. Murtaza, T.J. Meyer, J. Phys. Chem. 94 (1990) 239.
[139] K. Maruszewki, D.P. Stromman, J.R. Kincaid, J. Am. Chem. Soc. 115 (1993) 8345.
[140] C.R. Hecker, A.K.I. Gushurst, D.R. McMillan, Inorg. Chem. 30 (1991) 538.
[141] B.J. Coe, D.W. Thompson, C.T. Culbertson, J.R. Schoonover, T.J. Meyer, Inorg. Chem. 34 (1998) 3385.
[142] C.R. Hecker, P.E. Fanwick, D.R. McMillan, Inorg. Chem. 30 (1991) 659.
[143] A. Islam, N. Ikeda, A. Yoshimura, T. Ohno, Inorg. Chem. 37 (1998) 3093.
[144] D.P. Rillema, D.G. Taghdiri, D.S. Jones, C.D. Keller, L.A. Worl, T.J. Meyer, H.A. Levy, Inorg. Chem. 26 (1987) 578.
[145] K. Maruszewski, J.R. Kincaid, Inorg. Chem. 34 (1995) 2002.
[146] F. Barigelletti, L. DeCola, V. Balzani, R. Hag, J.C. Hassnoot, J. Reedyk, J.G. Vos, Inorg. Chem. 28 (1989) 4344.
[147] D.P. Rillema, C.B. Blanton, R.J. Shaver, D.C. Jackman, M. Boldaji, S. Bundy, L.A. Worl, T.J. Meyer, Inorg. Chem. 31 (1992) 1600.
[148] S.J. Milder, Inorg. Chem. 24 (1985) 3374.
[149] T. Ramasami, J.F. Endicott, G.H. Brubaker, J. Phys. Chem. 87 (1983) 5057.
[150] N.P. Ayala, C.M. Flynn, L.A. Sacksteder Jr., J.M. Demas, B.A. DeGraff, J. Am. Chem. Soc. 112 (1990) 2837.
[151] P. Reveco, R.H. Schmehl, W.R. Cherry, R.F. Fronczek, J. Selbin, Inorg. Chem. 24 (1985) 4078.
[152] W.F. Wacholtz, R.A. Auerbach, R.H. Schmehl, M. Ollino, W.R. Cherry, Inorg. Chem. 24 (1985) 1758.
[153] W.F. Wacholtz, R.A. Auerbach, R.H. Schmehl, Inorg. Chem. 25 (1986) 27.
[154] G.H. Allen, R.P. White, D.P. Rillema, T.J. Meyer, J. Am. Chem. Soc. 106 (1984) 2613.
[155] M. Hissler, A. Harriman, A. Khotyr, R. Ziessel, Chem. Eur. J. 5 (1999) 3366.
[156] G.J. Wilson, A. Launikonis, W.H.F. Sasse, A.W.-H. Mau, J. Phys. Chem. A 101 (1997) 4860.

[157] Y. Ohsawa, S. Sprouse, K.A. King, M.K. De Armond, K.W. Hanck, R.J. Watts, J. Phys. Chem. 91 (1987) 1047.
[158] D.E. Lacky, B.J. Pankuch, G.A. Crosby, J. Phys. Chem. 84 (1980) 2068.
[159] F. Barigelletti, L. DeCola, V. Balzani, R. Hage, J.G. Haasnoot, J. Reedijk, J.G. Vos, Inorg. Chem. 30 (1991) 641.
[160] R.S. Lumpkin, T.J. Meyer, J. Phys. Chem. 90 (1986) 5307.
[161] E.M. Kober, J.L. Marshall, W.T. Dressick, B.P. Sullivan, J.V. Caspar, T.J. Meyer, Inorg.Chem. 24 (1985) 2755.
[162] G. Denti, S. Serrone, L. Sabatino, M. Ciano, V. Ricevuto, S. Campagna, Gazz. Chim. Ital. 121 (1991) 37.
[163] M.E. Frink, P.C. Ford, L.H. Skibsted, Acta Chem. Scand. A38 (1984) 795.
[164] M. Nishizawa, T.M. Suzuki, S. Sprouse, R.J. Watts, P.C. Ford, Inorg. Chem. 23 (1984) 1837.
[165] M.T. Indelli, F. Scandola, Inorg. Chem. 29 (1990) 3056.
[166] L.J. McClure, P.C. Ford, J. Phys. Chem. 96 (1992) 6640.
[167] A. Islam, N. Ikeda, K. Nozaki, T. Ohno, J. Photochem. Photobiol. A 106 (1997) 61.
[168] F. Barigelletti, D. Sandrini, M. Maestri, V. Balzani, A. Von Zelewsky, L. Chassot, P. Jolliet, U. Maeder, Inorg. Chem. 27 (1988) 3644.
[169] M.A. Bergkamp, R.J. Watts, P.C. Ford, J. Am. Chem. Soc. 102 (1980) 2627.
[170] D.A. Sexton, L.H. Skibsted, D. Magde, P.C. Ford, Inorg. Chem. 23 (1984) 4533.
[171] D. Magde, L.H. Skibsted, Acta Chem. Scand. A41 (1987) 208.
[172] D. Magde, G.E. Rojas, L.H. Skibsted, Inorg. Chem. 27 (1988) 2900.
[173] L.H. Skibsted, Coord. Chem. Rev. 94 (1989) 151.
[174] L.H. Skibsted, M.P. Hancock, D. Magde, D.A. Sexton, Inorg. Chem. 23 (1984) 3735.
[175] L.H. Skibsted, M.P. Hancock, D. Magde, D.A. Sexton, Inorg. Chem. 26 (1987) 1708.
[176] M.A. Bergkamp, J. Brannon, D. Magde, R.J. Watts, P.C. Ford, J. Am. Chem. Soc. 101 (1979) 4549.
[177] G.A. Crosby, R.J. Watts, D.H.W. Carstens, Science 170 (1970) 1195.
[178] R.J. Watts, G.A. Crosby, Chem. Phys. Lett. 13 (1972) 619.
[179] K.A. King, F.O. Garces, S. Sprouse, R.J. Watts, in: H. Yersin, A. Vogler (Eds.), Photochemistry and Photophysics of Coordination Compounds, Springer, Berlin, 1987, p. 141.
[180] K.A. King, R.J. Watts, J. Am. Chem. Soc. 109 (1987) 1589.
[181] P.A. Anderson, G.B. Deacon, K.H. Haarman, F.R. Keene, T.J. Meyer, D.A. Reitsma, B.W. Skelton, G.F. Strouss, N.C. Thomas, Inorg. Chem. 34 (1995) 6145.
[182] A.P. Wilde, K.A. King, R.J. Watts, J. Phys. Chem. 93 (1991) 629.
[183] A.J. Lees, Comments Inorg. Chem. 17 (1995) 319.
[184] J.R. Schoonover, W.D. Bates, T.J. Meyer, Inorg. Chem. 34 (1995) 642.
[185] D.R. Striplin, G.A. Crosby, Chem. Phys. Lett. 221 (1994) 426.
[186] A.J. Lees, Chem. Rev. 87 (1987) 711.
[187] D.J. Stufkens, Comments Inorg. Chem. 13 (1992) 359.
[188] A. Juris, S. Campagna, I. Bidd, J.-M. Lehn, R. Ziessel, Inorg. Chem. 27 (1988) 4007.
[189] P.J. Giordano, M.S. Wrighton, J. Am. Chem. Soc. 101 (1979) 2888.
[190] L.A. Sacksteder, A.P. Zipp, E.A. Brown, J. Streich, J.N. Demas, B.A. DeGraff, Inorg. Chem. 29 (1990) 4335.
[191] L. Wallace, D.P. Rillema, Inorg. Chem. 32 (1993) 3836.
[192] A.P. Zipp, L.A. Sacksteder, J. Streich, A. Cook, J.N. Demas, B.A. DeGraff, Inorg. Chem. 32 (1993) 5629.
[193] L. Wallace, D.J. Jackman, D.P. Rillema, J.W. Merkert, Inorg. Chem. 34 (1995) 5210.
[194] J.R. Shaw, R.H. Schmehl, J. Am. Chem. Soc. 113 (1991) 389.
[195] F.W.H. Vankelmont, H.U. Güdel, M. Förtsch, H.B. Bürgi, Inorg. Chem. 36 (1997) 5512.
[196] G.F. Strouse, H.U. Güdel, Inorg. Chim. Acta 240 (1995) 453.
[197] M.M. Glezen, A.T. Lees, J. Am. Chem. Soc. 110 (1988) 3892.
[198] J.K. Hino, L. Della Ciana, W.J. Dressick, B.P. Sullivan, Inorg. Chem. 31 (1992) 1072.
[199] A.J. Rest, J.R. Sodeau, J. Chem. Soc. Faraday 2 (73) (1977) 1691.
[200] T.M. McHugh, R. Narayanaswamy, A.J. Rest, K. Salisbury, J. Chem. Soc. Chem. Commun. 1979, 208.
[201] R.M. Dahlgren, J.I. Zink, J. Am. Chem. Soc. 101 (1979) 1448.
[202] M.S. Wrighton, H.B. Abrahamson, D.L. Morse, J. Am. Chem. Soc. 98 (1976) 4105.
[203] A.J. Lees, A.W. Adamson, J. Am. Chem. Soc. 104 (1982) 3804.
[204] R.M. Dahlgren, J.I. Zink, Inorg. Chem. 18 (1979) 597.
[205] R.M. Kolodgiej, A.J. Lees, Organometallics 5 (1986) 450.
[206] M.S. Wrighton, D.L. Morse, J. Organomet. Chem. 97 (1975) 405.
[207] M.A. Bergkamp, R.J. Watts, P.C. Ford, J. Phys. Chem. 85 (1981) 684.
[208] R.T. Walters, A.W. Adamson, Acta Chem. Scand. A33 (1979) 53.
[209] J.F. Endicott, R.B. Lessard, Y. Lei, C.K. Ryu, R. Tamilarasan, ACS Symp. Ser. 307 (1986) 85.
[210] L. Vincze, D.A. Friesen, S.P. Mezyk, Inorg. Chem. 31 (1992) 4950.
[211] A.D. Kirk, D. Heyd, Inorg. Chem. 30 (1991) 2453.
[212] A. Ditze, F. Wasgestian, J. Phys. Chem. 89 (1985) 426.
[213] E. Zinato, A.W. Adamson, P. Riccieri, J. Phys. Chem. 89 (1985) 839.
[214] T. Dorfmüller, H. Dux, G. Fytas, W. Mersch, J. Chem. Phys. 71 (1979) 366.
[215] E. Zinato, Coord. Chem. Rev. 129 (1994) 195.
[216] E. Zinato, P. Riccieri, Coord. Chem. Rev. 125 (1993) 35.
[217] A. Pfeil, J. Am. Chem. Soc. 93 (1971) 5397.
[218] F.E. Lytle, D.M. Hercules, J. Am. Chem. Soc. 91 (1969) 253.
[219] L. Jacquet, A. Kirsch-De-Mesmaekes, J. Chem. Soc. Faraday 2 (88) (1992) 2471.
[220] A. Islam, N. Ikeda, K. Nozaki, Y. Okamoto, B. Gholamhass, A. Yoshimura, T. Ohno, Coord. Chem. Rev. 171 (1998) 355.
[221] L. DeCola, F. Barigelletti, M.J. Cook, Helv. Chim. Acta 71 (1988) 733.
[222] A.A. Bhuiyan, J.R. Kincaid, Inorg. Chem. 37 (1998) 2525.
[223] T. Norrby, A. Börye, B. Åkermark, L. Hammarstrõm, J. Alsins, K. Lasgari, R. Norrestam, J. Mårtensson, G. Stenhagen, Inorg. Chem. 36 (1997) 5850.
[224] W.R. Cherry, L.J. Henderson Jr., Inorg. Chem. 23 (1984) 983.
[225] E.G. Megehee, T.J. Meyer, Inorg. Chem. 28 (1989) 4084.
[226] W.S. Szulbinski, J.R. Kincaid, Inorg. Chem. 37 (1998) 859.
[227] A.W. Adamson, R.C. Fukuda, M. Larson, H. Mäcke, J.P. Puax, Inorg. Chim. Acta 44 (1980) L13.
[228] K.R. Barqawi, A. Llobet, T.J. Meyer, J. Am. Chem. Soc. 110 (1988) 7751.
[229] T.E. Keyes, J.G. Vos, J.A. Kolnaar, J.G. Haasnoot, J. Reedijk, R. Hage, Inorg. Chim. Acta 345 (1996) 237.
[230] E.M. Kober, Ph.D. thesis, University of North Carolina, 1982.
[231] I.M. Barclay, J.A.V. Butler, Trans Faraday Soc. 1938, 1445.
[232] A.T. Yeh, C.V. Shank, J.E. McCusker, Science 289 (2000) 935.
[233] L.S. Forster, Adv. Photochem. 16 (1991) 215.
[234] E.M. Kober, T.J. Meyer, Inorg. Chem. 23 (1984) 3877.
[235] T.R. Thomas, R.J. Watts, G.A. Crosby, J. Chem. Phys. 59 (1973) 2123.
[236] J.E. Hillis, M.K. DeArmond, J. Lumin. 4 (1971) 273.
[237] P. Spellane, R.J. Watts, Inorg. Chem. 32 (1993) 5633.
[238] D.M. Manuta, A.J. Lees, Inorg. Chem. 25 (1986) 1354.
[239] M.T. Indelli, A. Carioli, F. Scandola, J. Phys. Chem. 88 (1984) 2685.

[240] A.G. Joly, K.A. Nelson, J. Phys. Chem. 93 (1989) 2876.
[241] H.B. Ross, M. Boldaji, D.P. Rillema, C.B. Blanton, R.P. White, Inorg. Chem. 28 (1989) 1013.
[242] W.J. Vining, J.V. Caspar, T.J. Meyer, J. Phys. Chem. 89 (1985) 1095.
[243] H. Riesen, E. Krausz, J. Lumin. 62 (1994) 253.
[244] M. Licini, J.A.G. Williams, J. Chem. Soc. Chem. Commun. 1999, 1943.
[245] Y.S. Kang, F. Castelli, L.S. Forster, J. Phys. Chem. 83 (1979) 2868.
[246] K.F. Freed, Top. Appl. Phys. 15 (1976) 123.
[247] R. Englman, J. Jortner, Mol. Phys. 18 (1970) 145.
[248] R. Dellinger, M. Kasha, Chem. Phys. Lett. 36 (1975) 410.
[249] R. Dellinger, M. Kasha, Chem. Phys. Lett. 38 (1976) 9.
[250] R.B. Wilson, E.I. Solomon, Inorg. Chem. 17 (1978) 1729.
[251] D.J. Robbins, A.J. Thomson, Mol. Phys. 25 (1973) 1103.
[252] L.S. Forster, O. Mønsted, J. Phys. Chem. 90 (1986) 5131.
[253] H. Chernette, K. Bellefrough, A. Goursot, W.L. Waltz, Chem. Phys. Lett. 184 (1991) 282.
[254] F. Castelli, L.S. Forster, J. Am. Chem. Soc. 95 (1973) 7223.
[255] W. Targos, L.S. Forster, J. Chem. Phys. 44 (1966) 4342.